Marine and Petroleum Geology 102 (2019) 704–724

Contents lists available at ScienceDirect

Marine and Petroleum Geology

journal homepage: www.elsevier.com/locate/marpetgeo

Research paper

Characteristics and formation mechanism of multi-source mixed sedimentary rocks in a saline lake, a case study of the Permian Lucaogou Formation in the Jimusaer Sag, northwest China

Jingya Zhang[a,b,c,d], Guangdi Liu[a,b,*], Zhe Cao[a,b], Shizhen Tao[d], Maarten Felix[e], Yuhua Kong[f], Yiying Zhang[a,b]

[a] State Key Laboratory of Petroleum Resources and Prospecting, China University of Petroleum, Beijing, 102249, China
[b] College of Geosciences, China University of Petroleum, Beijing, 102249, China
[c] Collaborative Innovation Center of Unconventional Oil and Gas, China University of Petroleum, Beijing, 102249, China
[d] Research Institute of Petroleum Exploration & Development, PetroChina, Beijing, 100083, China
[e] NTNU Norwegian University of Science and Technology, Trondheim, 7491, Norway
[f] PetroChina Xinjiang Oilfield Company, Karamay, 834000, China

ARTICLE INFO

Keywords:
Lucaogou Formation
Tuffaceous material
Mixed sedimentary rocks
Mixing processes
Formation mechanism
Depositional models

ABSTRACT

The Permian Lucaogou Formation in the Jimusaer Sag of the southeastern Junggar Basin in China is an uncommon set of mixed sedimentary rocks. The mixed sediment content of the Lucaogou Formation is unusual due to the large amounts of tuffaceous material, which makes the system more complex than the commonly mixed siliciclastic-carbonate rocks. In this study, the volcanic material acts as a third end-member component in a multi-source mixed sedimentary system. Therefore, a new type of mixed siliciclastic-carbonate-tuffaceous rocks has been introduced.

Methods including core observations, thin section analysis, grain size measurements, and X-ray diffraction are used to investigate the characteristics of mineral components, sedimentary structures and lithological assemblages in upper and lower sections of the formation. These analyses are then used to determine the lateral distribution area of mixed sedimentation. Sedimentary mixing processes originally described for siliciclastic-carbonate systems are used and expanded here for the multi-source mixed rocks in a saline lacustrine basin. Controlling factors on mixed sedimentation included climate change, lake level fluctuation, tectonic activity and sediment supply rate mentioned in previous studies, as well as variations of energy levels in different parts of the lake. Mixed-depositional models for the lower and upper sections of the Lucaogou Formation in saline lacustrine basin have been established, respectively.

1. Introduction

The term mixed sediment normally refers to mixtures of siliciclastic materials and carbonates. Such mixtures form during deposition, either in one layer or as interfingering layers (Holmes, 1983; Tirsgaard, 1996). When such mixtures were first studied, it was assumed that carbonate production is reduced by an influx of siliciclastic material and that, for the most part, the two sediments do not deposit together. Later studies refined this assumption and described more complex mixed systems (e.g. Bruckner, 1953; Button and Vos, 1977; McIlreath and Ginsburg, 1982; Zhang and Ye, 1989; Brooks et al., 2003). Mixed siliciclastic-carbonate systems frequently develop on shelves and in platform settings, in both modern and ancient deposits (Dorsey and Kidwell, 1999; Testa and Bosence, 1999; Purdy and Gischler, 2003; Page, 2006; Gischler et al., 2010). The distribution of siliciclastics and of carbonates is governed by different processes, and as a result, the mixtures of these vary across the depositional environments. The siliciclastic sediment is introduced into the system predominantly by rivers, while the carbonate sediment production takes place in situ in shallow marine or lacustrine environments (Caracciolo et al., 2013; Accordi and Carbone, 2016). The carbonate production is controlled by a variety of physical, chemical and biological processes, which vary throughout the shallow marine and lake environments (Choi and Ginsburg, 1982; Flood and Orme, 1988; Pilkey et al., 1988).

Mount (1984) identified four sedimentary mixing processes on rimmed carbonate platforms by studying mixed siliciclastic and

* Corresponding author. State Key Laboratory of Petroleum Resources and Prospecting, China University of Petroleum, Beijing, 102249, China.
E-mail address: lgd@cup.edu.cn (G. Liu).

https://doi.org/10.1016/j.marpetgeo.2019.01.016
Received 6 July 2018; Received in revised form 11 November 2018; Accepted 14 January 2019
Available online 21 January 2019
0264-8172/

carbonate sediments in shallow shelf environments of more than 150 modern and ancient examples. He divided the mixing processes into four general categories: punctuated mixing, facies mixing, in situ mixing, and source mixing. This classification has been widely used in subsequent research (e.g. Li, 2008; Zhao et al., 2013). Following this model, different mixing sedimentation types were proposed based on the characteristics in different areas (Dorsey and Kidwell, 1999; Zhang, 2000; Wang, 2001; Dong et al., 2007, 2009; Ding et al., 2013). Various depositional architecture models of mixed siliciclastic-carbonate rocks have been developed (Mack and James, 1986; Dorsey and Kidwell, 1999; Wright et al., 2005; GarcÍa-Hidalgo et al., 2007; Reis and Suss, 2016) that describe vertical and lateral facies assemblages and cyclic sequences of mixed sedimentation. These changes are caused by varying sedimentation and subsidence rates, eustatic sea level changes and climate changes (Yose and Heller, 1989; Einsele, 1996; Wright et al., 2005). Compared with shallow marine mixed siliciclastic-carbonate sediments, lacustrine mixed sedimentary systems have been studied less well, especially saline lacustrine environments. Existing studies mainly focus on the reservoir characteristics of lacustrine mixed rocks (Palermo et al., 2008; Feng et al., 2013), rarely on the mixing characteristics and formation mechanisms. In terms of lithology, the carbonate components in mixed sedimentary systems in previous studies (Orpin et al., 2004; Isaack et al., 2016; Lubeseder et al., 2009; Yose and Heller, 1989) are mainly limestone (bioclastic packstone/wackestone/grainstone, micrite, oolites, marl and marginal reef in modern sediments), while mixed siliciclastic-dolomitic sequences have been paid less attention before (Escalona and Abud, 1989; Wu et al., 2016).

The rocks of the Lucaogou Formation were deposited in a saline lacustrine siliciclastic-dolomitic mixed system (Wu et al., 2016), where in addition large amounts of volcanic material were deposited, making the mixed system more complicated. In this setting, the syngenetic and penecontemporaneous dolomicrite was produced in a saline lacustrine basin, mixed with terrigenous clastic sand, silt, and with transported tuffaceous materials, and thus formed a mixed system of three end-member components.

Previous studies indicate that the Lucaogou Formation was deposited mainly in shallow near-shore to semi-deep lacustrine environments and partially in a delta front environment (Cao et al., 2016; Wu et al., 2016; Qiu et al., 2016). The main lithologies are dark mudstones, fine sandstones, siltstones, dolomicrite, dolarenite, limestone, tuff and some transitional lithologies (dolomitic siltstone, dolomitic mudstone, calcareous dolomite, etc.) (Si et al., 2013; Jiang et al., 2015).

In this study, the petrological characteristics of the Lucaogou Formation mixed rocks are discussed systematically and a previously undocumented type of mixed sedimentary rocks (sliciclastic-carbonate-tuffaceous) is introduced by taking the Lucaogou Formation as an example. A combination of petrological, mineralogical and granulometry analysis was employed to systematically investigate the classification system, lithological assemblages, lateral and vertical distribution characteristics, mixing processes and mixed depositional models.

2. Geological setting

The Junggar Basin, located in northwestern China, is a large intracontinental superimposed basin. It has experienced multi-stage tectonic movements, including, from oldest to youngest, Hercynian, Indosinian, Yanshanian and Himalayan movements. In the southeast of the basin lies the Jimusaer Sag, covering an area of 1278 km^2 (Fig. 1a). This sag is a dustpan-shaped depression, which is bounded by a steep fault in the west and more gently dipping faults around the rest of the basin (Fig. 2). The sag is separated from the Beisantai Uplift by the Xidi Fault and the Laozhuangwan Fault in the west, from the Shaqi Uplift by the Jimusaer Fault in the north, and bordered by the Fukang Fault in the south and by the Guxi Uplift in the east (Fig. 1b). Seven Carboniferous-Permian volcanic edifices were present on the Beisantai Uplift (Mao et al., 2012), and delivered volcanic sediments to the basin. The basin is underlain by Middle Carboniferous folded basement, and filled with Permian to Quaternary sedimentary sequences, which dip gently towards the west (Fig. 2). The Middle Permian in the Jimusaer Sag can be divided into three formations (Cao et al., 2017b), which are, from base to top: the Wulabo, the Jingjingzigou and the Lucaogou Formation (Fig. 1c).

The Lucaogou Formation is widespread across the whole area, and has an average vertical thickness of 200–350 m, and a maximum thickness of up to 500 m (Kuang et al., 2013). It can be divided into two members, the lower section (P_2l_1) and the upper section (P_2l_2); the boundary between the two sections is formed by a maximum flooding surface (Cao et al., 2017a). It can be further divided into four sand groups, $P_2l_1^2$, $P_2l_1^1$, $P_2l_2^2$, and $P_2l_2^1$ upwards (Fig. 3). The Lucaogou Formation in the Jimusaer Sag was deposited in a saline lacustrine environment (Kuang et al., 2012; Wu et al., 2016). The deposits are overall fine-grained and characterized by thin layers and frequently alternating lithologies (Kuang et al., 2012; Cao et al., 2017a). Mixed rocks are mostly present in the upper part of $P_2l_1^2$ and $P_2l_2^2$, containing terrigenous clastic grains, carbonate components and tuffaceous materials.

3. Samples and experiments

A total of 89 core samples from nine wells in the Jimusaer Sag have been investigated in detail (Fig. 1), among which 48 samples cover the lower section of the Middle Permian Lucaogou Formation, and 41 samples cover the upper section. Petrological and mineralogical analyses of the samples were carried out at the State Key Laboratory of Petroleum Resources and Prospecting, China University of Petroleum. The analyses include core and thin section observation, X-ray diffraction mineralogical analysis (XRD), and granulometry analysis of the core samples.

3.1. Petrological and mineralogical analysis

After core description, samples from cores were made into polished circular briquettes of one-inch diameter for petrographic examination. Alizarin Red-S dye was added in the thin sections for determination of calcite. Thin sections were studied using a Leica DM4500 microscope equipped with LED illumination and a LAS V4.2 digital camera detection system. Thin sections were analyzed under transmitted white light and reflected white light. Mineral constituents of core samples were analyzed using a Bruker D2 PHASER X-ray diffraction instrument, whose emissive and receiving slits are 0.6 mm and 8 mm respectively. The diffractometer was equipped with a Cu-target Ceramic X-ray tube, operating at 30 kV and 10 mA. Samples were step-scanned from 6° to 50° with a step size of 0.02°(2θ). The lithology and mineral composition of the samples are listed in Table 1.

3.2. Granulometry analysis

Grain size parameters, one of the most basic and important characteristics of clastic rocks (Zhao and Zhu, 2001; Yang et al., 2013), can be used in the interpretation of paleo-depositional environments (Krumbein, 1938; Visher, 1969; Stapor and Tanner, 1975; Friedman and Sanders, 1978; Christiansen et al., 1984; Peng et al., 2005; Ghoshal et al., 2010; Roux and Rojas, 2007). Here the characteristics of grain size distribution, cumulative grain-size curves and some parameters were used to estimate the relative energy of the sedimentary environments where the mixed rocks were deposited.

Twenty-three sandstone and siltstone samples were selected and successively pretreated with 10 ml 30% H_2O_2 to remove organic matter, 5 ml 10% HCl to remove calcium carbonate, and 300 mg $Na_4P_2O_7{\cdot}10H_2O$ to further separate the grains (following the procedures of Konert and Vandenberghe, 1997; Cao et al., 2017a). The grain size distribution was measured with a Mastersizer 2000 laser diffraction

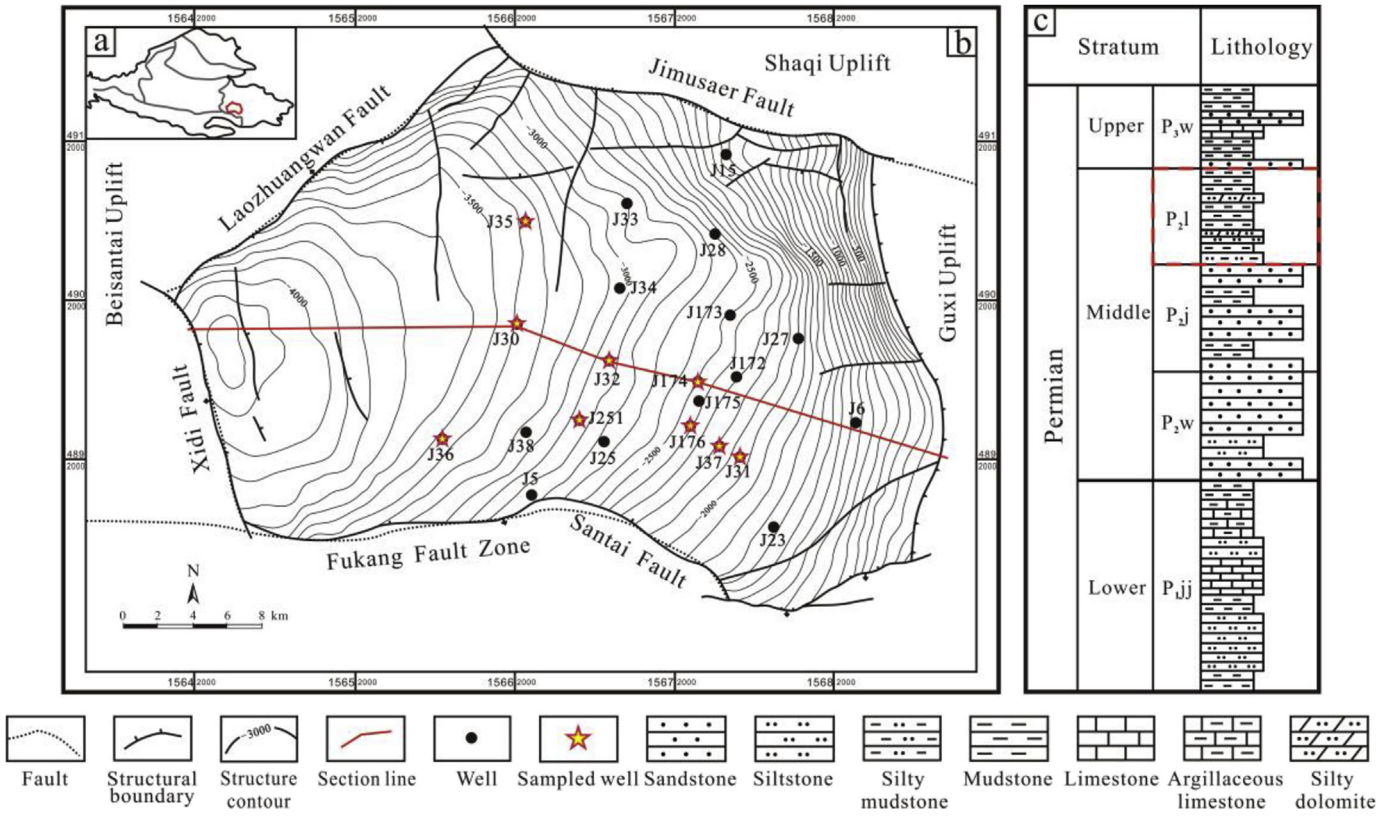

Fig. 1. Location map and Permian stratigraphic column of the Jimusaer Sag in the Junggar Basin. (a) Location map of the Jimusaer Sag in the Junggar Basin; (b) Structural framework and major wells in the Jimusaer Sag; (c) The stratigraphic column of Permian strata; the Lucaogou Formation (P_2l) is at the top of Middle Permian. Red line is location of seismic profile shown in Fig. 2. (For interpretation of the references to color in this figure legend, the reader is referred to the Web version of this article.)

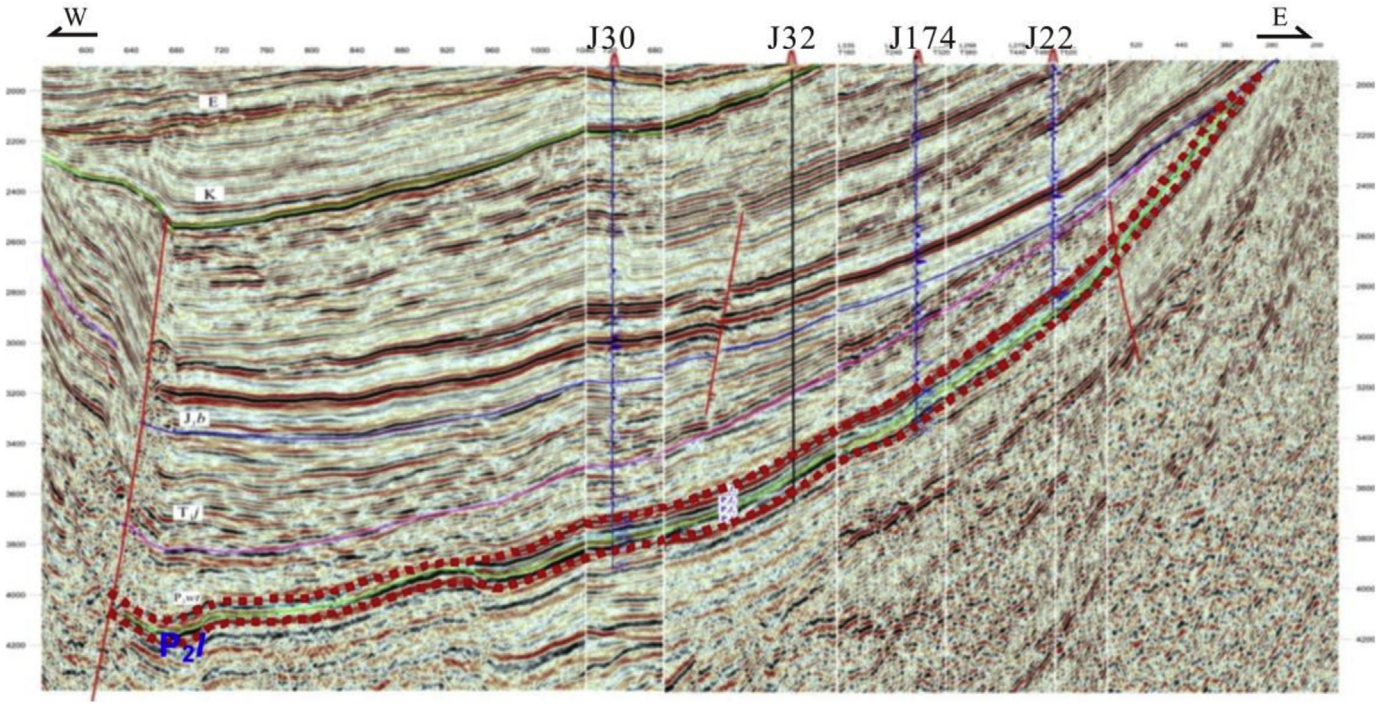

Fig. 2. Seismic profile showing that the Jimusaer Sag is a dustpan-shaped Sag. The location of the seismic profile is shown in Fig. 1. The Lucaogou Formation (P_2l) is located between the red dotted lines. (For interpretation of the references to color in this figure legend, the reader is referred to the Web version of this article.)

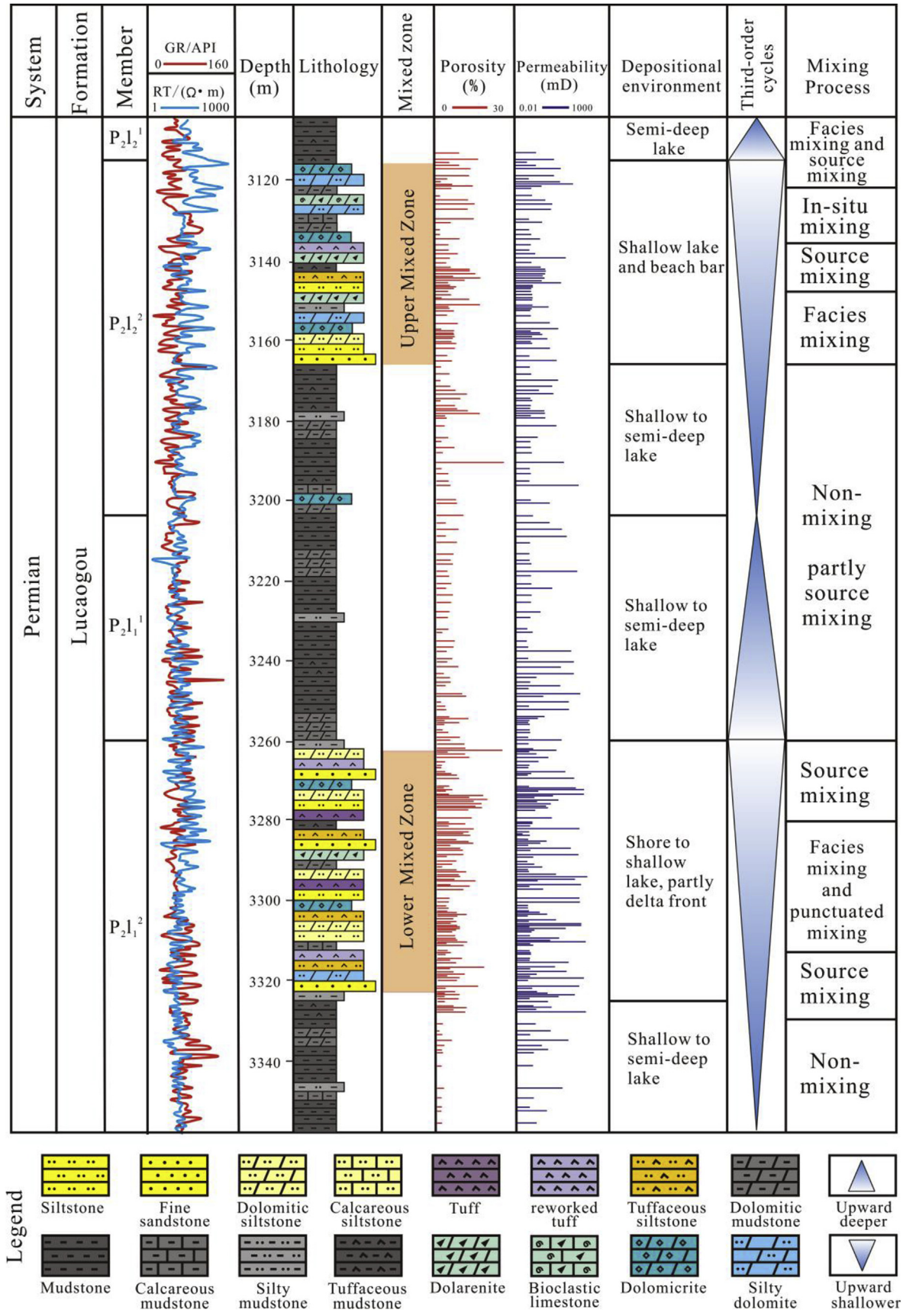

Fig. 3. Composite columnar section of the Permian Lucaogou Formation in Well J174, Jimusaer Sag (modified after Wu et al., 2016).

Table 1
Mineral composition of the main lithologies in the Lucaogou Formation, Jimusaer Sag, determined by XRD analysis.

Well	Depth (m)	Section	Lithology	Quartz (%)	K-feldspar (%)	Plagioclase (%)	Q+K+P (%)	Calcite (%)	Dolomite (%)	Ankerite (%)	C+D+A (%)	Clay (%)	Siderite (%)	Pyrite (%)	Analcime (%)	Anhydrite (%)
J176	3028.32	Upper	Dark mudstone	38.5	6	13.5	58	3	3.6	–	6.6	35.5	–	–	–	–
J176	3030.3	Upper	Tuff	39.4	4.1	33.7	77.2	2.2	5.2	–	7.4	8.4	–	7	–	–
J176	3034.7	Upper	Dolomicrite	14.1	–	9.3	23.4	–	76.6	–	76.6	–	–	–	–	–
J176	3035.95	Upper	Tuff	35.4	8.1	22	65.5	8.4	13.2	–	21.6	11.3	1.6	–	–	–
J176	3039.32	Upper	Dark mudstone	23.9	16.6	24.4	64.9	9.3	–	–	9.3	23.1	2.6	–	–	–
J176	3042	Upper	Dark mudstone	26.5	4.7	34.5	65.7	4.3	–	–	4.3	30	–	–	–	–
J176	3048.33	Upper	Dolomitic siltstone	19.2	–	43.3	62.5	15.8	–	20.3	36.1	1.5	–	–	–	–
J176	3049	Upper	Dolarenite	11.1	1.3	12.8	25.2	–	70.4	–	70.4	4.4	–	–	–	–
J176	3053.94	Upper	Silty mudstone	23.9	5.5	28.7	58.1	5.5	–	13.9	19.4	22.4	–	–	–	–
J251	3598.15	Upper	Silty mudstone	31.7	3.9	35.5	71.1	1.9	25.6	–	27.5	1.4	–	–	–	–
J251	3604.06	Upper	Calcareous mudstone	31.7	4.1	27.9	63.7	24	–	3.1	27.1	5.1	–	4.1	–	–
J251	3623.18	Upper	Argillaceous siltstone	29.5	3.9	40.2	73.6	2.6	–	17.6	20.2	6.3	–	–	–	–
J251	3627	Upper	Calcareous fine sandstone	16.2	–	56.4	72.6	11.6	–	13.3	24.9	2.5	–	–	–	–
J251	3627.28	Upper	Dolomitic siltstone	19.4	4.3	49.3	73	13.8	–	6.8	20.6	4.6	–	1.9	–	–
J251	3628.62	Upper	Calcareous fine sandstone	18.3	–	58.1	76.4	13	–	7.8	20.8	2.1	–	–	–	0.8
J251	3628.65	Upper	Calcareous fine sandstone	18.9	3	58.2	80.1	12.7	–	4.3	17	2.9	–	–	–	–
J251	3628.75	Upper	Dolomitic fine sandstone	21.3	2.8	46.6	70.7	4	–	21.7	25.7	3.8	–	–	–	–
J251	3629.31	Upper	Dolomitic siltstone	25.8	3.5	42.6	71.9	4.4	–	22.6	27	1.1	–	–	–	–
J251	3629.45	Upper	Dolomitic fine sandstone	20.7	3.5	23.9	48.1	2.3	–	37	39.3	6.8	5.9	–	–	–
J251	3629.5	Upper	Calcareous fine sandstone	21.9	3	26.4	51.3	1.3	35.6	–	36.9	11.8	–	–	–	–
J251	3629.55	Upper	Silty limestone	22.9	4.2	39	66.1	33.3	–	–	33.3	0.6	–	–	–	–
J251	3630.1	Upper	Dolomicrite	17.7	1.9	27.7	47.3	1.9	48.7	–	50.6	2	–	–	–	–
J251	3635.2	Upper	Calcareous mudstone	20.9	5.8	8	34.7	28.5	–	5.2	33.7	31.6	–	–	–	–
J31	2712.61	Upper	Dolomicrite	21.5	1.6	4.2	27.3	1.5	71.3	–	72.8	–	–	–	–	–
J31	2716.28	Upper	Dolomicrite	22.7	0.9	7.1	30.7	–	69.3	–	69.3	–	–	–	–	–
J31	2717.9	Upper	Tuffaceous siltstone	37.4	3.3	39	79.7	1.5	3.1	–	4.6	11.5	–	4.1	–	–
J31	2719.1	Upper	Dolomitic mudstone	24.6	1.9	12.7	39.2	1.9	–	44.2	46.1	13.9	–	–	–	0.7
J31	2722.75	Upper	Tuff	30.5	3.5	22.7	56.7	2.5	–	12.4	14.9	8.9	–	–	19.5	–
J31	2723.88	Upper	Reworked tuff	40.7	10.2	31.6	82.5	4.9	–	5.1	10	5.8	1.7	–	–	–
J31	2773	Upper	Silty limestone	14.4	1.6	24.3	40.3	47.1	9.7	–	56.8	1.3	–	1.6	–	–
J31	2789.35	Upper	Calcareous siltstone	20.4	3.9	27.3	51.6	15.8	8.7	–	24.5	23.9	–	–	–	–
J32	3567.57	Upper	Tuffaceous siltstone	24.3	8.7	42.8	75.8	6	–	5.8	11.8	7.5	5	–	–	–
J32	3568	Upper	Silty tuff	27.9	10	36.5	74.4	5	–	7.8	12.8	8.6	4.2	–	–	–
J32	3569.18	Upper	Tuffaceous siltstone	27.8	17.2	30.4	75.4	8.2	–	11.4	19.6	5	–	–	–	–
J32	3570.32	Upper	Silty mudstone	19.8	–	26.2	46	11.8	–	22.1	33.9	10.2	9.9	–	–	–
J32	3572.13	Upper	Dolomitic Tuff	28.7	–	32.8	61.5	8.9	–	10.1	19	13.1	6.5	–	–	–

(*continued on next page*)

Table 1 (*continued*)

Well	Depth (m)	Section	Lithology	Quartz (%)	K-feldspar (%)	Plagioclase (%)	Q+K+P (%)	Calcite (%)	Dolomite (%)	Ankerite (%)	C+D+A (%)	Clay (%)	Siderite (%)	Pyrite (%)	Analcime (%)	Anhydrite (%)
J32	3573.13	Upper	Tuff	21.7	7.2	28	56.9	11.3	–	–	11.3	22.1	9.7	–	–	–
J37	2845.79	Upper	Tuffaceous siltstone	35.8	9.8	28.7	74.3	4.4	4.6	–	9	16.7	–	–	–	–
J37	2846.95	Upper	Tuffaceous siltstone	30.9	10	20.8	61.7	7	14	–	21	17.2	–	–	–	–
J37	2859.09	Upper	Silty dolomite	23.8	3.1	31.1	58	–	31.4	–	31.4	10.6	–	–	–	–
J37	2866.72	Upper	Dolarenite	12.1	1.7	19.5	33.3	17.5	–	45.1	62.6	0.2	–	3.9	–	–
J176	3170.45	Lower	Silty dolomite	22.1	2.5	19.8	44.4	3.9	39.4	–	43.3	12.2	–	–	–	–
J176	3172.52	Lower	Silty mudstone	31.1	4.9	24.5	60.5	2.7	19.6	–	22.3	17.1	–	–	–	–
J176	3173.12	Lower	Dolomitic mudstone	29.3	5.4	23.3	58	–	27.3	–	27.3	13.6	1.1	–	–	–
J176	3173.35	Lower	Silty mudstone	27.6	4.3	24	55.9	–	29.3	–	29.3	14.8	–	–	–	–
J176	3174.75	Lower	Dolomitic siltstone	23.9	3.8	32.4	60.1	–	31.9	–	31.9	8	–	–	–	–
J176	3177.42	Lower	Tuff	25.1	4.9	23.6	53.6	4.7	25.2	–	29.9	16.6	–	–	–	–
J176	3178.2	Lower	Silty mudstone	29.2	4.7	31.9	65.8	–	12.4	–	12.4	21.8	–	–	–	–
J251	3728.81	Lower	Calcareous mudstone	24.8	2.8	20.6	48.2	38.8	2.8	–	41.6	10.2	–	–	–	–
J251	3731.51	Lower	Calcareous fine sandstone	16.7	2.3	32.5	51.5	38.6	–	1.4	40	4.6	–	3.9	–	–
J251	3731.8	Lower	Calcareous fine sandstone	12.4	2.1	42.2	56.7	37.7	1.5	–	39.2	4.2	–	–	–	–
J251	3733.69	Lower	Dolomicrite	12	1.4	12.9	26.3	8	54.5	–	62.5	11.2	–	–	–	–
J251	3738.68	Lower	Silty dolomite	14	3.2	22.8	40	–	47.2	–	47.2	7.2	–	5.6	–	–
J251	3739.06	Lower	Dolomitic mudstone	29.2	4.3	28.7	62.2	–	29.6	–	29.6	8.3	–	–	–	–
J251	3742.98	Lower	Silty dolomite	32.5	3	24.5	60	–	33.8	–	33.8	6.2	–	–	–	–
J251	3745.82	Lower	Argillaceous siltstone	34	6.4	36.4	76.8	1.4	8	–	9.4	6.7	–	7.2	–	–
J251	3749.86	Lower	Dolomitic tuff	22.3	6.5	31.9	60.7	5	14.6	–	19.6	17.4	2.4	–	–	–
J251	3751	Lower	Argillaceous siltstone	38.3	6.7	32.5	77.5	1.6	4.6	–	6.2	11.5	–	4.9	–	–
J251	3751.99	Lower	Dolomitic siltstone	34.9	7.7	34.8	77.4	1.8	18	–	19.8	2.8	–	–	–	–
J251	3753.85	Lower	Calcareous siltstone	25.4	7.6	48.6	81.6	2.3	8.5	–	10.8	7.6	–	–	–	–
J251	3754.15	Lower	Dolomitic siltstone	25.2	5.6	37.7	68.5	5.3	17.7	–	23	8.5	–	–	–	–
J251	3755.45	Lower	Silty dolomite	28.7	3	24.5	56.2	6.3	34.3	–	40.6	3.2	–	–	–	–
J251	3755.55	Lower	Silty dolomite	35.6	3.2	21.9	60.7	7.8	29.6	–	37.4	2	–	–	–	–
J251	3758.15	Lower	Dolomicrite	8.4	2.2	20.2	30.8	6.2	60.4	–	66.6	2.7	–	–	–	–
J251	3758.45	Lower	Dolomitic siltstone	21.4	8.1	30.2	59.7	2	30.5	–	32.5	5.8	1.8	–	–	–
J251	3758.85	Lower	Calcareous siltstone	17.8	5	53.1	75.9	10.7	6.4	–	17.1	5.5	–	1.5	–	–
J251	3759.15	Lower	Dolomitic siltstone	24.2	5.8	43.1	73.1	1.5	12.4	–	13.9	9.4	–	3.6	–	–
J251	3764.96	Lower	Calcareous siltstone	22.9	5.3	20.8	49	33.4	8.3	–	41.7	5.4	1.8	2.2	–	–
J251	3765.25	Lower	Calcareous siltstone	21.6	5.5	27	54.1	32	3.6	–	35.6	4.2	–	6.2	–	–
J251	3765.55	Lower	Silty limestone	29.6	3.5	11.2	44.3	41	12.4	–	53.4	2.2	–	–	–	–
J251	3768.69	Lower	Calcareous Siltstone	21.7	3.9	41.3	66.9	19.5	–	–	19.5	11.4	–	2.3	–	–

(*continued on next page*)

Table 1 (*continued*)

Well	Depth (m)	Section	Lithology	Quartz (%)	K-feldspar (%)	Plagioclase (%)	Q+K+P (%)	Calcite (%)	Dolomite (%)	Ankerite (%)	C+D+A (%)	Clay (%)	Siderite (%)	Pyrite (%)	Analcime (%)	Anhydrite (%)
J251	3770.41	Lower	Silty dolomite	27.4	3.3	19.3	50	5.4	38.2	–	43.6	4.9	1.6	–	–	–
J251	3771.15	Lower	Dolomicrite	14.4	3.6	25.7	43.7	–	42.8	–	42.8	11.9	–	–	–	1.5
J31	2851.41	Lower	Calcareous siltstone	28.5	3.7	53.1	85.3	9.2	–	–	9.2	5.4	–	–	–	–
J31	2897.7	Lower	Silty dolomite	16.9	1.6	24.3	42.8	–	37.7	–	37.7	10.9	–	8.6	–	–
J31	2898.07	Lower	Silty mudstone	38.3	3.6	28.8	70.7	–	25.7	–	25.7	3.6	–	–	–	–
J32	3724.91	Lower	Reworked tuff	31.7	7.5	40	79.2	–	15	–	15	5.8	–	–	–	–
J32	3725.32	Lower	Dolomitic siltstone	34.4	6.9	27.5	68.8	–	22.7	–	22.7	8.4	–	–	–	–
J32	3729.2	Lower	Dolomitic siltstone	25.9	4.7	30.6	61.2	–	29.5	–	29.5	9.3	–	–	–	–
J32	3731.25	Lower	Dolomitic siltstone	28.2	4.8	36.7	69.7	–	22.2	–	22.2	8	–	–	–	–
J32	3732.35	Lower	Dolomitic tuff	25.7	5	44.6	75.3	–	20.1	–	20.1	4.5	–	–	–	–
J35	4074.13	Lower	Dolomitic mudstone	23.8	2.7	17.1	43.6	–	39.1	–	40.5	15.9	–	–	–	–
J35	4074.6	Lower	Dolomitic siltstone	22.4	3.5	25.7	51.6	10	20	–	30	18.4	–	–	–	–
J35	4076.03	Lower	Silty mudstone	24.9	6	32.8	63.7	11	4.7	–	15.7	20.6	–	–	–	–
J35	4079.03	Lower	Dolomitic siltstone	33.6	5.8	31.9	71.3	1.4	23.6	–	25	3.7	–	–	–	–
J35	4089.82	Lower	Silty mudstone	17.9	2.9	26.1	46.9	16.9	–	14.4	31.3	21.8	–	–	–	–
J36	4214.09	Lower	Dolarenite	15.2	2.2	20.1	37.5	21.4	–	29.9	51.3	2.5	3.8	–	4.9	–
J36	4216.09	Lower	Dolomitic siltstone	25.9	3	24.5	53.4	8.3	28.2	–	36.5	8.4	1.7	–	–	–
J36	4216.28	Lower	Calcareous siltstone	25	3.3	34.9	63.2	16.1	12.4	–	28.5	6.4	–	1.9	–	–

Explanation: Q+K+P = Quartz+K-feldspar+Plagioclase; C+D+A = Calcite+Dolomite+Ankerite.

Table 2
Grain size parameters for fine sandstone and siltstone samples in the Lucaogou Formation, Jimusaer Sag.

NO.	Well	Depth(m)	Lithology	Md/um	Mz/um	σ1	Sk_1	K_G
1	J176	3174.75	Dolomitic siltstone	39.22	31.43	2.37	0.20	0.98
2	J176	3174.75	Dolomitic siltstone	38.77	30.89	2.39	0.20	0.98
3	J251	3751.99	Dolomitic siltstone	57.96	41.90	2.39	0.30	0.94
4	J251	3754.15	Dolomitic siltstone	73.54	50.85	2.38	0.35	0.99
5	J32	3725.32	Dolomitic siltstone	69.74	51.49	2.43	0.28	0.98
6	J32	3731.25	Dolomitic siltstone	66.89	52.70	2.34	0.27	0.94
7	J251	3759.15	Dolomitic siltstone	54.84	39.96	2.18	0.34	1.00
8	J36	4216.09	Dolomitic siltstone	71.45	50.85	2.18	0.37	1.02
9	J251	3629.55	Calcareous siltstone	92.07	55.36	2.28	0.49	1.01
10	J251	3765.25	Calcareous siltstone	56.20	36.75	2.28	0.40	0.92
11	J31	2851.41	Calcareous siltstone	70.84	44.22	2.13	0.50	0.97
12	J36	4216.28	Calcareous siltstone	64.87	46.89	2.01	0.39	1.09
13	J251	3764.96	Calcareous siltstone	37.32	27.97	2.37	0.22	1.16
14	J251	3758.85	Calcareous siltstone	55.44	40.33	1.93	0.38	1.07
15	J251	3745.82	Argillaceous siltstone	84.68	61.30	2.42	0.32	1.00
16	J251	3751.00	Argillaceous siltstone	63.80	45.54	2.39	0.31	1.02
17	J31	2717.9	Tuffaceous siltstone	73.40	53.39	2.26	0.37	1.04
18	J251	3627	Calcareous fine sandstone	95.31	63.59	1.91	0.52	1.13
19	J251	3628.62	Calcareous fine sandstone	83.07	55.60	1.91	0.51	1.12
20	J251	3731.8	Calcareous fine sandstone	100.53	76.73	1.59	0.48	1.49
21	J251	3731.51	Calcareous fine sandstone	119.62	96.79	1.50	0.49	1.86
22	J251	3629.45	Dolomitic fine sandstone	99.69	69.42	1.86	0.50	1.31
23	J251	3628.75	Dolomitic fine sandstone	91.28	56.53	2.20	0.49	1.02

Md = median size; Mz = mean size; σ1 = standard deviation; Sk_1 = skewness; K_G = kurtosis.

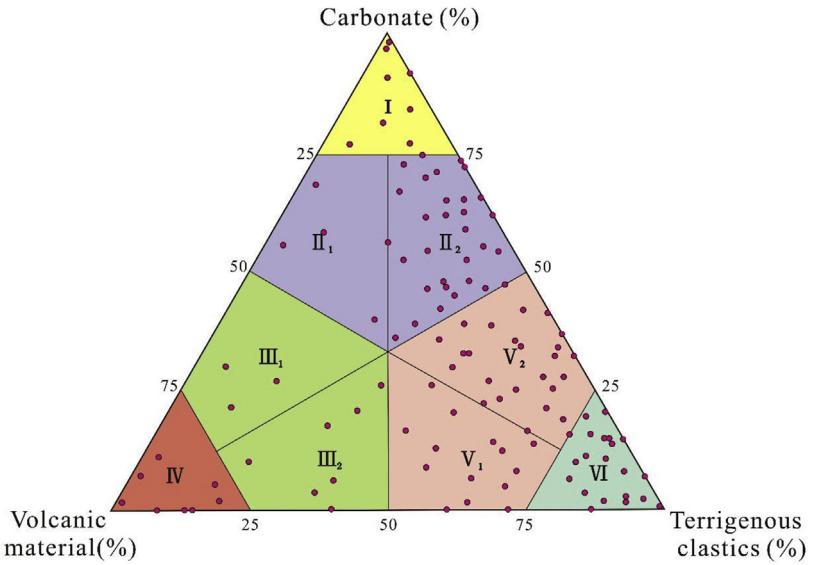

Fig. 4. Classification system for mixed siliciclastic-carbonate-tuffaceous rocks of Lucaogou Formation, Jimusaer Sag. The red dots are the samples from the cores. (For interpretation of the references to color in this figure legend, the reader is referred to the Web version of this article.)

instrument (Malvern Instruments Ltd, UK) with 100 bins ranging from 0.02 to 2000 μm.

The grain size parameters used here are mean grain size (Mz) and standard deviation (σ1). These parameters are listed in Table 2 and were calculated according to the equations in Folk and Ward (1957). Some of the measurements used here have been published in Cao et al. (2017a). The mean grain size is influenced by source of supply and overall energy of the depositional environment (Folk, 1966; Zhu, 2008). The standard deviation (σ1) is used as a measure of uniformity or sorting degree of particles (Hatch and Choate, 1929; Folk, 1966; Amireh, 2015).

3.3. Naming of rock types

The names of lithologies used here have been determined as follows: first, the relative content (in percentage) of three components (terrigenous clastics, carbonate and volcanic material) was calculated. Second, if the content of all three components is lower than 75%, the nomenclature of mixed rocks is determined by the component of the highest relative content, and the component of second highest content is considered as well. For example, if there is 56% carbonate, 28% terrigenous clastics, and 16% tuffaceous material in a mixed rock, it is called terrigenous siliceous carbonate. Further, the specific type of mineral components (e.g. calcite or dolomite in carbonate), grain size characteristics (e.g. mud, silt or sand), and sedimentary structure (e.g.

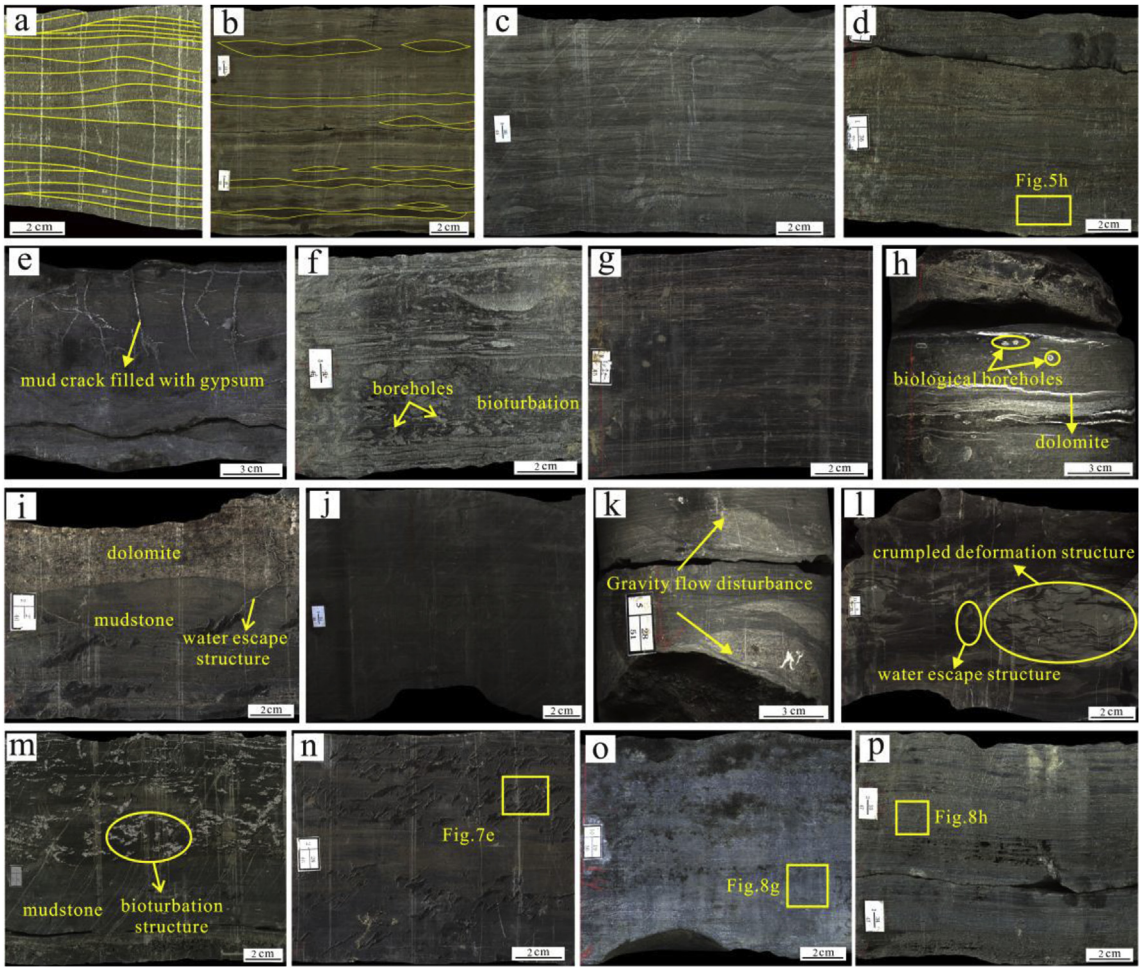

Fig. 5. Core photos of lithologies and sedimentary structures of the Lucaogou Formation, Jimusaer Sag. Thin section images of some of these deposits are shown in the figures indicated next to the yellow squares. (a) wavy bedding and ripple cross lamination in siltstones (J37, 2867.35m); (b) flaser bedding and lenticular bedding in argillaceous siltstones (J31, 2896.69m); (c) flaser bedding and lenticular bedding in argillaceous siltstones (J31, 2861.71); (d) tuffaceous siltstone (J32, 3567.57m); (e) mud crack filled with gypsum in silty mudstone (J176, 3178.88m); (f) bioturbation and burrows filled with silts in mudstone (J31, 2860.24m); (g) horizontal bedding in silty mudstone (J174, 3149.4m); (h) dolomite laminae and some vertical and sloping biological boreholes in dark mudstones (J174, 3111.11m); (i) interbedding of mudstone and dolomite (J30, 4053.51m); (j) massive bedding in dark mudstones (J31, 2862.97m); (k) siltstone or fine-sandstone body deposited in mudstone by gravity flow, probably a slump (J174, 3122.11m); (l) crumpled deformation structure caused by slumping and water-escape structure caused by compaction (J174, 3338.29m); (m) bioturbation, partly parallel to bedding and partly perpendicular to bedding in dark mudstone (J30, 4151.68m); (n) boundstone (J30, 4053.78m); (o) tuff (J176, 3177.42m); (p) weak horizontal bedding structure in reworked tuff (J31, 2717.9m). (For interpretation of the references to color in this figure legend, the reader is referred to the Web version of this article.)

tuff or reworked tuff) are taken into account as well. If there is 43% dolomite and 13% calcite in the 56% carbonate minerals mentioned above, and 20% silt-sized grains and 8% mud-sized grains in the 28% terrigenous clastic component, then the mixed rock is called silty dolomite. On the other hand, if any component has a relative content higher than 75%, then the rock was named according to the component of the highest content. For example, a rock with 82% terrigenous clastics, 14% carbonate components, and 4% volcanic materials is called a terrigenous clastic rock. Furthermore, the texture of rocks was also taken into consideration when a name is given and the terrigenous clastic rock can be classified into fine sandstone, siltstone and mudstone. The names of rock types are determined by XRD data combined with petrological characteristics from thin section description.

4. Results

4.1. Classification of lithologies

Core and thin-section observations show that the lithologies in the Lucaogou Formation vary frequently at millimeter scale or even at micrometer scale (Figs. 5 and 6). Therefore, the lithological characteristics are very complicated. The mixed sedimentary rocks here have been classified into three categories: terrigenous-dominated mixed rocks, carbonate-dominated mixed rocks, and tuffaceous-dominated rocks. They are further divided into nine types according to the terminology above (Fig. 4). In all, more than 20 specific types of rock are recognized according to their mineral components, sedimentary structure and texture (Fig. 4).

With regard to rock samples with a single component, the carbonate rocks include dolarenite, dolomicrite and boundstone; the volcanic rocks include tuff and reworked tuff; and the terrigenous clastic rocks include pebbly sandstone, dolomitic fine sandstone, siltstone, argillaceous siltstone, silty mudstone and dark mudstone. Other rock samples are from transitional lithological facies with two or more end-member components. The ternary plot of Fig. 4, showing the classification of all analyzed samples, shows that the transitional/mixed rock types are more common than those with a single component, which is a typical characteristic of mixed sedimentary rocks. Among all the transitional lithologies, the mixed siliciclastic-carbonate rocks, especially mixed siliciclastic-dolomitic rocks are the most common mixture in the

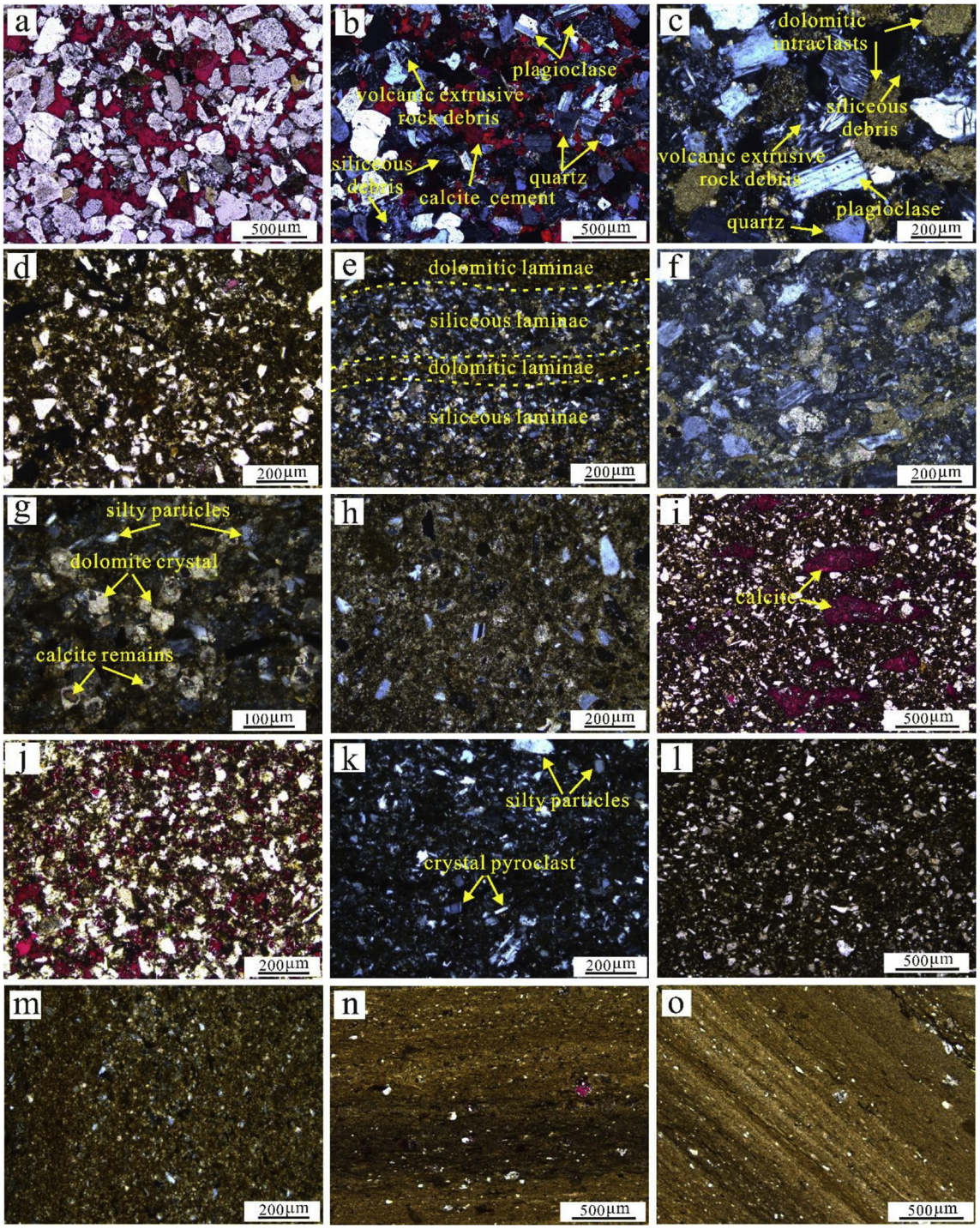

Fig. 6. Optical photomicrographs of components and textures of different kinds of terrigenous-dominated mixed rocks in the Lucaogou Formation, Jimusaer Sag. In brackets after the description are the well number, section, and depth in core. (PPL = plane-polarized light; CPL = cross-polarized light) (a) calcite cement in fine sandstone, which is very common, PPL, (J251, P_2l_1, 3731.51m); (b) the components of grains and cements in calcareous fine sandstone, same as (a), with CPL; (c) the components of grains in dolomitic fine sandstone, CPL, (J251, P_2l_2, 3628.75m); (d) argillaceous siltstone, CPL, (J251, P_2l_1, 3751m); (e) dolomitic laminae alternating with siliceous laminae, CPL, (J176, P_2l_1, 3174.75m); (f) dolomitic rock debris mixed with silty particles in dolomitic siltstone, CPL, (J251, P_2l_2, 3627.28m); (g) subhedral to euhedral rhombic dolomite crystals with a size of 20–50 μm mixed irregularly with similar-sized terrigenous clastic particles in dolomitic siltstones, some calcite remains are found in the center of dolomite crystals, CPL, (J36, P_2l_1, 4216.09m); (h) silt-sized terrigenous clasts scattered and embedded in mud-sized dolomite matrix in dolomitic siltstone, CPL, (J251, P_2l_1, 3758.45m); (i) rock debris of calcite deposited together with silty siliciclastic grains in calcareous siltstone, PPL, (J251, P_2l_1, 3765.25m); (j) calcite cement in calcareous siltstone, PPL, (J251, P_2l_1, 3764.96m); (k) tuffaceous siltstone, CPL, (J32, P_2l_2, 3567.57m); (l) silty mudstone, PPL, (J176, P_2l_1, 3178.2m); (m) mud-sized dolomite matrix and microcrystalline dolomite mixed with clay minerals in dolomitic mudstone, CPL, (J35, P_2l_1,4074.13m); (n) calcite in calcareous mudstone, PPL, (J251, P_2l_2, 3635.2m); (o) horizontal bedding in dark mudstone (J176, P_2l_2, 3028.32m).

Lucaogou Formation (Fig. 4).

The mixture of volcanic material and terrigenous clastics is also common through the Lucaogou Formation, which is named as silty tuff and tuffaceous siltstone (Fig. 4). However, the mixed carbonate-tuffaceous lithological assemblage is of limited occurrence (Fig. 4), with only a small number of samples of dolomitic tuff and tuffaceous dolomite.

4.2. Facies

The facies characteristics are as follows.

4.2.1. Pebbly sandstone

Small amounts of pebbly sandstone develop at the bottom of the Lucaogou Formation and it is found in the cores of Well J15 (Shao et al., 2015). The pebbly sandstone is offwhite to grey, poorly sorted and rounded, with gravels directional in it. It is interpreted to have been deposited in a delta, which is the highest energy environment in this system.

4.2.2. Fine sandstone

There are two types of fine sandstones in the Lucaogou Formation in the Jimusaer Sag, calcareous fine sandstone and dolomitic fine sandstone, both of which are grey (Fig. 6a–c). If there is no carbonate in it, we just call it fine sandstone. The terrigenous clastic grains in fine sandstone are usually angular to subangular, and the matrix is a mixture of argillaceous and dolomite mud. The cement is calcite and there are small amounts of cryptocrystalline silica in pore spaces (Fig. 6a–c). The grain size distribution of fine sandstone is unimodal with a narrow main peak at fine sand sized grains (Fig. 7a and b). The grains are moderately sorted (Table 2). The cumulative grain size curves of two types of fine sandstone show a “bi-segment” pattern, consisting of suspended loads and saltation components (Inman, 1952; Zhu, 2008) with the boundary around 0.11 mm (Fig. 8a and b). Very fine and fine sand were transported as saltation load, while finer silt-sized grains were suspended load, indicating current action of relatively weak to moderate intensity.

The specific characteristics of the two types of fine sandstones are as follows.

4.2.2.1. Calcareous fine sandstone. The grains in calcareous fine sandstone mainly consist of quartz, plagioclase, and various clastic rock debris: siliceous debris and volcanic extrusive rock debris (Fig. 6a and b). A large amount of calcite cement frequently developed between the clastic particles, and is found filling up pores where grains are in contact, or as inlaid cement (Fig. 6a and b). There is relatively little interstitial material in calcareous fine sandstone. The XRD data show that the average value of the sum of quartz, K-feldspar and plagioclase can reach up to 67.7%, and the average content of calcite is 17.7%. The content of dolomite and ankerite is 5.3% and 3.8%, respectively, and there is less than 5% of clay minerals (Fig. 9).

The grain size distribution and sorting of the calcareous fine sandstone show a relatively energetic environment of deposition compared to most other sediment types in the Lucaogou Formation, and indicate deposition in a delta.

4.2.2.2. Dolomitic fine sandstone. The grain components of dolomitic fine sandstone also consist mainly of quartz, feldspar and rock debris, and a large amount of dolomitic intraclasts occur frequently (Fig. 6c). Some of them have experienced diagenesis of metasomatism and recrystallization in a late burial stage, and formed ankerite crystals (Fig. 6c, Table 1). The siliciclastic grains are (sub)angular, while the carbonate clasts are rounded (Fig. 6c). Calcite and microcrystalline ankerite cements can be seen in pore spaces. The matrix is primarily argillaceous, dolomite mud and small amounts of cryptocrystalline silicon with a total content of about 10%.

The XRD data show that the average contents of quartz, K-feldspar and plagioclase in dolomitic fine sandstones are 21%, 3.1% and 35.2%, respectively and the average content of ankerite is up to 29.3%. Compared with calcareous fine sandstone, the calcite content of dolomitic fine sandstones is much lower, at only 3.15%. The content of clay minerals is 5.3%.

In general, the terrigenous clastic components are compositionally and texturally immature, indicating a type of deposit that is near to the source, possibly at a delta front.

4.2.3. Siltstone

Siltstone is one of the most common lithologies in the Lucaogou Formation. The color of siltstone ranges from light grey to dark grey (Fig. 5a–d). Many kinds of sedimentary structures develop in siltstones, including wavy bedding (Fig. 5a), ripple cross lamination (Fig. 5a), flaser bedding and lenticular bedding (Fig. 5b and c). There are four

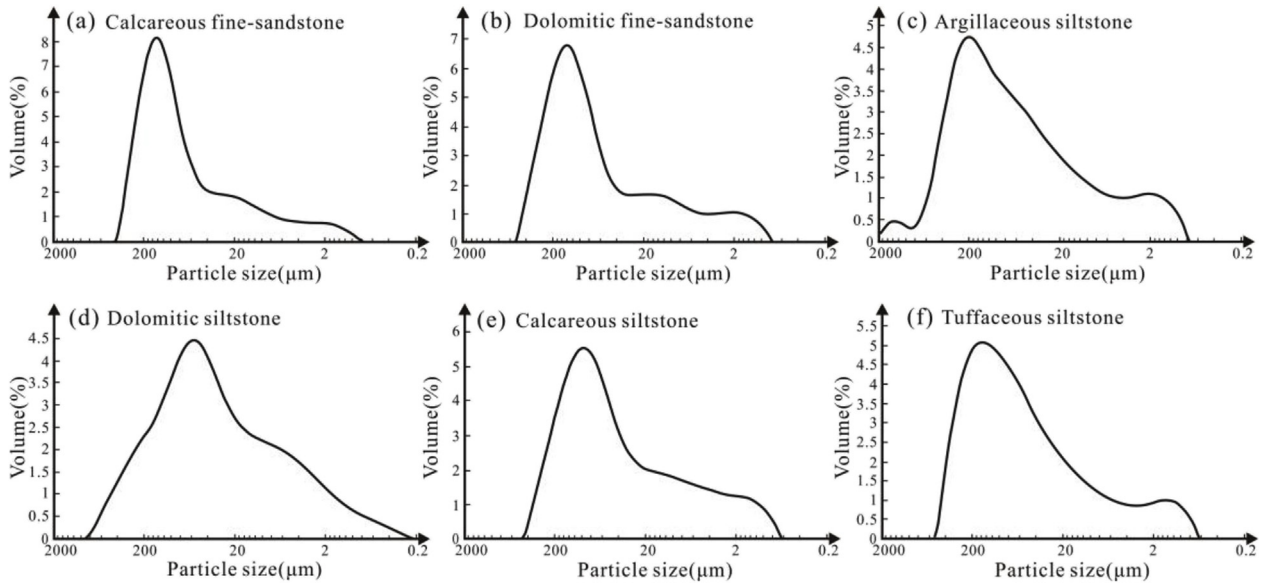

Fig. 7. Representative grain-size frequency distribution patterns of Lucaogou fine sandstone and siltstone samples. Well number and depth in core: (a) J251, 3627m; (b) J251, 3628.75m; (c) J251, 3745.82m; (d) J176, 3174.75m; (e) J251, 3765.25m; (f) J31, 2717.9m.

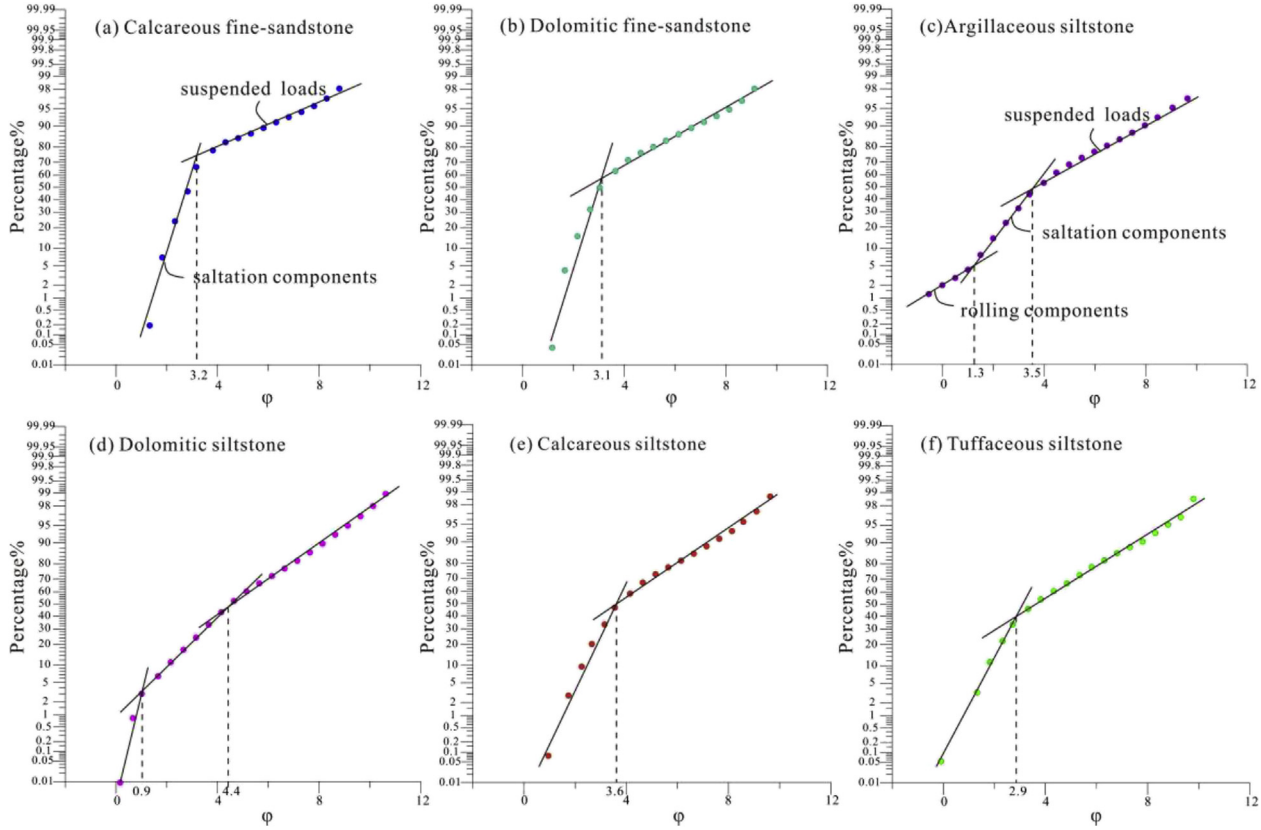

Fig. 8. Cumulative grain-size curves of Lucaogou fine sandstones and siltstones in Jimusaer Sag. Well number and depth in core: (a) J251, 3731.51m; (b) J251, 3629.45m; (c) J251, 3751m; (d) J176, 3174.75m; (e) J36, 4216.28m; (f) J31, 2717.9m .

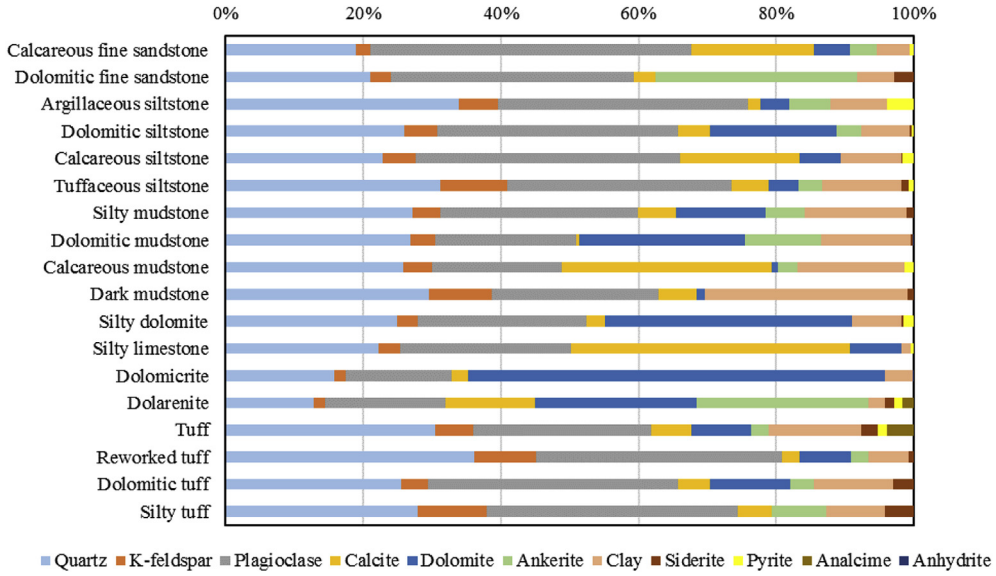

Fig. 9. Mineral composition and content of the mixed sedimentary rocks in the Lucaogou Formation, Jimusaer Sag.

types of siltstones: argillaceous siltstone, dolomitic siltstone, calcareous siltstone and tuffaceous siltstone (Fig. 6d–k). The silica grains in siltstone consist mostly of quartz, rock debris and some subhedral alkali-feldspar and plagioclase. The interstitial material including matrix and cements in pore spaces varies for the different types of siltstone. The standard deviation values of the grain size indicate poor to very poor sorting (Table 2). The characteristics of each facie are described below.

4.2.3.1. Argillaceous siltstone. The matrix of argillaceous siltstones has a relatively high content of clay minerals, and a small amount of mud-grade dolomite. The matrix was deposited together with a large amount of quartz and subhedral plagioclase and alkali-feldspar grains. Some calcite cement is found in argillaceous siltstones (Fig. 6d). XRD data show that the contents of quartz, K-feldspar and plagioclase are 33.9%, 5.7% and 36.4%, respectively, accounting for more than 70% of the total content. Carbonate minerals in argillaceous siltstones can reach to 12%, and the average content of clay minerals and pyrite is 8.2% and 4%, respectively (Table 1, Fig. 9).

The grain size distribution of argillaceous siltstones is unimodal with a main peak at silt-sized grains, but another weak peak at mud-sized grains (Fig. 7c). The cumulative grain size curves of argillaceous siltstones show a "tri-segment" pattern (Fig. 8c), indicating about 52% suspended loads, 44.2% saltation components, and 3.8% rolling components, respectively, with boundaries of 0.41 mm and 0.09 mm (Fig. 8c). This means that medium sand was transported as rolling components, very fine and fine sand as saltation load and finer silt-sized grains as suspended load. The poor sorting indicates a short transport distance.

Flaser bedding and lenticular bedding can commonly be seen in argillaceous siltstones (Fig. 5b and c), indicating deposition in a shallow lake, maybe influenced by water flow.

4.2.3.2. Dolomitic siltstone. This is one of the most common mixed rocks, in which terrigenous supply is more dominant than the intrabasinal carbonate component. XRD data show that the total content of quartz, K-feldspar and plagioclase is 67%, and the average value of clay minerals in dolomitic siltstones is 7.4%. The content of carbonate is about 25%, of which the dolomite accounts for nearly 20% (Fig. 9).

Sedimentary structures include wavy bedding and wave ripple cross-bedding. When the facie is laminated, dolomite laminae frequently alternates with siliceous laminae in dolomitic siltstones (Fig. 6e). Siliceous grains are found disorderly mixing with dolomite minerals (Fig. 6f–h). The silty grains are subangular, indicating that they have experienced short-distance transportation before mixing with dolomite.

There are three occurrences of dolomitic siltstone according to the morphological characteristics of dolomite according to thin section observation (Fig. 6f–h). The first one is dolomitic clasts mixed with silty particles (Fig. 6f). Mud-grade aragonite and calcite with high Mg^{2+} content was replaced by dolomite just after deposition, when the unconsolidated or semi-consolidated dolomite was broken into dolomitic clasts, transported and deposited with silt-sized siliciclastic grains. During the diagenesis of metasomatism and recrystallization in the late burial stage, some of the dolomitic debris turned into bigger ankerite crystals (Fig. 6f). The second occurrence of dolomitic siltstone is as subhedral to euhedral rhombic dolomite crystals with a size of 20–50 μm which have point or line contacts with similar-sized terrigenous clastic particles (Fig. 6g). Some of them have calcite remains in the interior part, indicating incomplete replacement of dolomite (Fig. 6g). The euhedral-subhedral crystal structures are typical characteristics of burial dolomite, mainly in the shallow burial stage (Wang et al., 2010; Sibley and Gregg, 1987). Another type of dolomitic siltstone is as silt-sized terrigenous clasts scattered and embedded in mud-sized dolomite matrix or microcrystalline dolomite as a result of replacement of magnesian calcite just after deposition (in the penecontemporaneous period) (Fig. 6h).

The grain size distribution of dolomitic siltstones is unimodal (Fig. 7d). The cumulative grain size curves show a "tri-segment" pattern (Fig. 8d), indicating about 52% suspended loads, 43%～45.4% saltation components, and 2.5%～5% rolling components, respectively. The grains are poorly sorted (Table 2). Dolomitic siltstone often developed in shore to shallow lake during facies mixing process (see discussion). The sedimentary structures indicate that they formed in relatively energetic conditions or oscillatory water movement (Nichols, 2009).

4.2.3.3. Calcareous siltstone. Calcareous siltstone is less common than dolomitic siltstone in the Lucaogou Formation. Some subangular interclasts of calcite deposited together with silty siliciclastic grains, and experienced recrystallization later (Fig. 6i). The matrix of calcareous siltstone contains a relatively large amount of clay minerals and a small amount of mud-grade dolomite. Some calcite cement developed in calcareous siltstone, and is distributed between or replaces part of the silty grains (Fig. 6j).

The XRD data show that the sum of quartz, K-feldspar and plagioclase content can reach up to 63%. The average calcite content is up to 18.5%, and that of dolomite is 6.8%. The content of clay minerals ranges from 4.2% to 23.9%, with an average value of 9.2% (Fig. 9).

The grain size distribution curves of calcareous siltstones are similar to those of dolomitic siltstone (Fig. 7e), but the cumulative grain size curves show a "bi-segment" pattern: suspended loads and saltation components with a boundary at 0.08 mm (Fig. 8e). The grains in calcareous siltstone are poorly sorted (Table 2).

Calcareous siltstone was deposited in a shore to shallow lake environment. Compared with dolomitic siltstone, it often formed in water with lower salinity.

4.2.3.4. Tuffaceous siltstone. Alternating thin laminae can be seen in core samples of tuffaceous siltstones (Fig. 5d). Tuffaceous siltstone consists mainly of fine-grained silty particles and some volcanic ash (Fig. 6k). The silty particles are mainly composed of angular to subangular quartz, feldspar and lithic debris. The tuffaceous material consists mainly of tiny crystal pyroclasts and vitric pyroclasts (Fig. 6k). XRD data show that the content of quartz and feldspar is up to 70%, and clay minerals which formed through devitrification vary from 1.5% to 17.2%. The average content of dolomite and ankerite is 3.1% and 6.8%, respectively (Fig. 9).

The grain size distribution of tuffaceous siltstones is unimodal with a main peak at silt-sized grains, but another weak peak at mud-sized grains (Fig. 7f). The cumulative grain size curves of tuffaceous siltstones show a "bi-segment" pattern (Fig. 8f), indicating suspended loads of 52%～60% and saltation components of 40%～48% with a boundary at 0.13 mm. The grains are poorly sorted.

This type of rock is not indicative of a specific environment, but represents a mixing process of material from two sources, terrigenous and volcanic tuffaceous material, which can place in different parts of the lake.

4.2.4. Mudstone

Mudstone is one of the most common fine-grained sedimentary rocks that accounts for more than half of the total thickness of the Lucaogou Formation (Si et al., 2013). The mudstone can be classified into silty mudstone, dolomitic mudstone, calcareous mudstone, and dark mudstone (Fig. 6l–o).

4.2.4.1. Silty mudstone. The silty mudstone is grey to dark grey (Fig. 5e–g). It consists of a clay mineral matrix and small amounts of mud-sized carbonate minerals, with scattered subangular silt grains of quartz, feldspar and debris of terrigenous rocks (Fig. 6l). A small amount of dolomite cement in subeuhedral or rhombic crystals developed in silty mudstone. XRD data show that the sum of quartz, K-feldspar and plagioclase content ranges from 46% to 71.1%, with an average value of 60%, and the content of clay minerals ranges from 1.4% to 22.4%. The average content of carbonate minerals is 5.53% calcite, 13.03% dolomite and 5.6% ankerite (Fig. 9).

Silty mudstone with different sedimentary structures developed in different parts of the lake. Mud cracks filled with gypsum can be found in some of the silty mudstones (Fig. 5e), and would have formed when shallow parts of the lake were dry. When the shallow areas flooded again, water of high salinity filled in the cracks and some gypsum precipitated in them (Fig. 5e). Therefore, the silty mudstone with mud cracks formed in shore or shallow lake environments. Bioturbation and burrows can be seen in some of the silty mudstones (Fig. 5f), indicating strong biological activity when it deposited, likely in a shallow lake environment. Mudstones with horizontal bedding or massive bedding formed in the semi-deep lake (Fig. 5g).

4.2.4.2. Dolomitic/calcareous mudstone. Compared with silty mudstone, dolomitic/calcareous mudstone has a darker color. The difference between dolomitic mudstone and calcareous mudstone is the type and occurrence of carbonate minerals. XRD data show that the average

content of siliceous minerals in both kinds of mudstone is almost 50%. However, there are 30.4% calcite, 0.9% dolomite and 2.8% ankerite in calcareous mudstone, and 0.5% calcite, 24% dolomite and 11.1% ankerite in dolomitic mudstone (Fig. 9). The content of clay minerals in calcareous and dolomitic mudstone is 15.6% and 12.9%, respectively.

Dolomitic mudstone is composed of microcrystalline dolomite and clay minerals (Fig. 6m). The micro-structure of dolomite in dolomitic mudstone is mud-sized dolomite matrix or microcrystalline dolomite (Fig. 6m). On the macro level, some dolomite laminae can be found in this type of mudstone (Fig. 5h), and some dolomite developed just after the deposition of dark mudstone (Fig. 5i). In calcareous mudstone, the calcite always developed as cement or as replacement of silica grains (Fig. 6n). Massive bedding and horizontal bedding can be seen in dolomitic/calcareous mudstone (Fig. 6n). Calcareous/dolomitic mudstone often developed in low energy shallow to semi-lake environments.

4.2.4.3. Dark mudstone. Dark mudstone is dark grey to grey black and contains massive and horizontal bedding (Fig. 5i-l). The grains in dark mudstone are mostly mud-sized siliciclastic clasts and clay minerals. According to XRD data, the mineral components of dark mudstone consist of quartz, K-feldspar and plagioclase with a total content of 63%, 5.53% calcite, 1.2% dolomite, and clay minerals up to nearly 30% (Table 1, Fig. 9). No tuff could be identified in the mudstone by microscopic investigation, but it is likely that some tuffaceous material is included given the widespread distribution of windblown tuff across the lake.

Some fossils such as bivalve and palaeoniscus also can be found in dark mudstones. Sedimentary structures include massive and horizontal bedding (Figs. 5j and o), gravity flow disturbances (Fig. 5k), dolomite laminae (Fig. 5h), some crumpled deformation structures caused by slumping (Fig. 5l), water-escape structures caused by compaction (Fig. 5i and l), vertical and sloping biological boreholes (Fig. 5h), and bioturbation structure (Fig. 5m). Generally, dark mudstone formed under quiet hydrodynamic conditions in semi-deep lacustrine environments.

4.2.5. Boundstone

The color of boundstone is dark grey or grey black (Fig. 5n). This type of rock often forms in situ, and can be algal dolomite or carbonates, after the death of creatures. The boundstone appears oriented (Figs. 4k and 10a), showing certain effect of lake waves. It often occurs as stripped interlayers of one to 5 cm in mudstone (Fig. 7e), indicating relatively quiet and shallow depositional condition and maybe in shallow lake.

4.2.6. Silty dolomite

This type of rock is distributed widely throughout the strata. The characteristics of silty dolomite are similar to dolomitic siltstones, but silty dolomite contains more dolomite minerals, nearly 40% (Table 1, Fig. 9). The occurrences of dolomite in this type of rocks are mainly of two types (Fig. 10b and c). One is as subhedral to euhedral rhombic dolomite crystals with a size of 20–50 μm, mixed randomly with terrigenous clastics such as plagioclase, quartz, K-feldspar, and sometimes some kinds of rock debris (Fig. 10b). Some remains of calcite can be observed in the interior of dolomite crystals (Fig. 10b), implying replacement of calcite by dolomite during metasomatic diagenesis. The other type of silty dolomite consists of terrigenous clastic grains scattered in mud-grade or microcrystalline dolomite (Fig. 10c). Silty dolomite contains more carbonate minerals than silty grains, suggesting that intrabasinal material is a more important source than terrigenous supply. The mixture of the two indicates that it often developed in shore to shallow lacustrine environments, where both sources can provide material.

4.2.7. Silty limestone

This type of rock is not common in the Lucaogou Formation. The calcite mineral in silty limestone is mud to silt-sized carbonate crystals with poor crystal shape. The siliciclastic grains are scattered among the calcareous components (Fig. 10d). Quartz and plagioclase account for half of the total content in silty limestone. The content of calcite ranges from 33.3% to 41%, and that of clay minerals is very low with an average value of only 1.4% (Fig. 9). Silty limestone often developed in a shallow lake environment, under similar conditions as the silty dolomite.

4.2.8. Tuffaceous dolomite

This type of rock indicates a mixing process of two sources: volcanic material and carbonate components. It is not common in the Lucaogou Formation, with only a few samples of this type (Fig. 4). In the early stage, fine-grained calcium carbonate (lime mud) precipitated from lake water, and was replaced by dolomite before or after the deposition of volcanic material. Therefore, some tuffaceous material dropped in the lake, and some tiny crystal pyroclasts mixed with fine-grained dolomite, and were cemented by calcite or ankerite later. The main mineral components of tuffaceous dolomite are dolomite, quartz, and plagioclase, with small amounts of calcite, clay minerals and ankerite.

4.2.9. Dolomicrite

The content of dolomite in dolomicrite, on average 60.5%, but sometimes up to 90% (Fig. 9, Table 1). The content of quartz and feldspar minerals is more than 30%, while the content of clay minerals is lower than 5%. The dolomite crystal in dolomicrite is micritic or silt-sized crystal of 5–15 μm (Fig. 10e and f).

This type of dolomite usually has not experienced strong recrystallization (Huang et al., 1997), and forms through dolomitization just after deposition in a saline lacustrine environment with strong evaporation (Gregg and Shelton, 1990; Fu et al., 2006; Loyd and Corsetti, 2010), which is also shown by the presence of anhydrite (Fig. 10g). The dolomicrite formed in quiescent parts of the shore to shallow lake.

4.2.10. Dolarenite

There are many types of carbonate grain in dolarenite, including bioclasts, ooids and intraclasts (Fig. 10h and i). XRD data show that the average content of carbonate in dolarenite is 61.4% (calcite 12.97%, dolomite 23.5% and ankerite 25%), and the content of quartz, K-feldspar and plagioclase is 32%. Traces of clay, siderite and pyrite are also detected in dolarenite (Fig. 9). The grains are cemented by rhombic dolomite or ankerite, and sparry calcite cements later (Fig. 10h and i).

Dolarenite formed when previously deposited biotic components or semi-consolidated carbonate sediments mixed with mud were broken and reworked by water flow or lake waves, transported for a certain distance, and deposited again. At the same time, some terrigenous clastic particles brought in by the river mixed with them. This type of rock often formed in an environment with high energy, in the nearshore lake or shallow lake areas.

4.2.11. Tuff and reworked tuff. Tuff and reworked tuff are distributed widely in the entire Lucaogou Formation, but they developed more commonly in the lower section (Jiang et al., 2015). The color of this type of rock is grey to dark grey in core samples (Fig. 5o–p).

Microscopic phenomena show that large amounts of angular volcanic crystal debris and a matrix of fine-grained tuffaceous particles can frequently be seen in the Lucaogou Formation (Fig. 11). The crystal debris has a wide grain size range from 30 to 200 μm with a regular shape and intact edge, but some of them show cracking grains and embayed dissolution structures (Fig. 11a and b). The crystal debris consists mainly of quartz, plagioclase and alkali feldspar including orthoclase, albite and a minor amount of sanidine (Fig. 11a–c). In addition, lithoclasts of extrusive rocks with doleritic structure can be

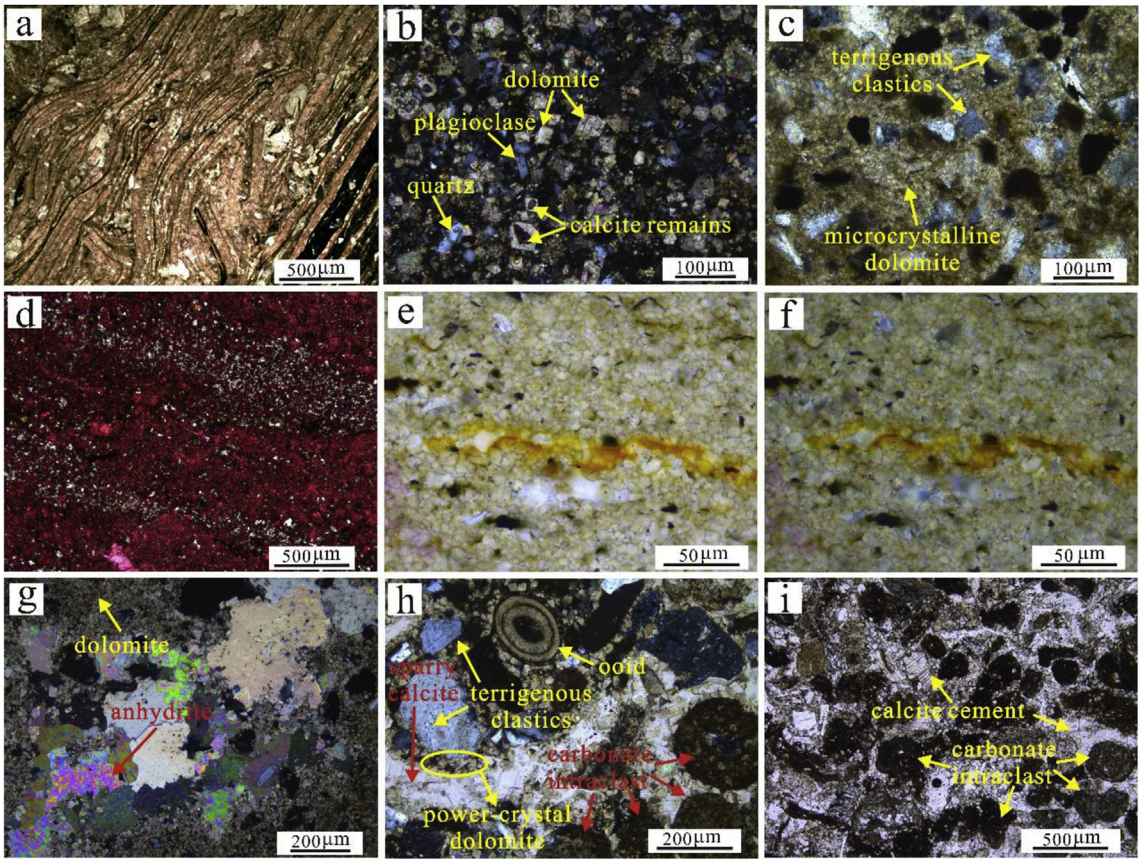

Fig. 10. Photomicrographs of different carbonate-dominated mixed rocks in the Lucaogou Formation, Jimusaer Sag. In brackets after the description are the well number, section, and depth in core.
(PPL = plane-polarized light; CPL = cross-polarized light) (a) boundstone (J30, P_2l_2, 4053.78m); (b) silty dolomite, the euhedral-subhedral dolomite crystals show point-contact with terrigenous grains, and calcite remains can be observed in the interior of dolomite crystals, CPL, (J176, P_2l_1, 3170.45m); (c) silty dolomite, terrigenous clastic grains scattered in microcrystalline dolomite, CPL, (J31, P_2l_1, 2897.7m); (d) silty limestone, PPL, (J251, P_2l_1, 3764.96m); (e) dolomicrite, PPL, (J31, P_2l_2, 2716.28m); (f) dolomicrite, same as (e), with CPL, (J31, P_2l_2, 2716.28m); (g) anhydrite in dolomite, CPL, (J251, P_2l_1, 3758.45m); (h) dolarenite, sand-sized carbonate intraclasts admixed with siliceous grains, CPL, (J37, P_2l_2, 2866.72m); (i) dolarenite, carbonate intraclasts cemented by calcite, PPL, (J37, P_2l_2, 2866.72m).

observed in thin sections (Fig. 6a–c, 11c), demonstrating that volcanic material in the Lucaogou Formation comes from intermediate-basic magma.

The main mineral components of tuff and reworked tuff are quartz, feldspar and amorphous silica. XRD data show that the average content of quartz and feldspar can reach up to 67%, the content of carbonate is about 16% and clay mineral content is relatively low with an average of 11.3% (Fig. 9). A high content of analcime, considered to be related to volcanic activities, was also detected in some tuff samples (Fig. 9, Table 2). Thin section analysis showed that the tuffaceous material has experienced devitrification, and some of it was replaced by carbonate (Fig. 11b–d, 11g-h).

The plagioclase that came from intermediate-basic magma in both crystal pyroclasts and matrix kept its euhedral lath-shaped and acicular crystal form (Fig. 11a–d), indicating that most of the volcanic material has probably not been transported by water flow, but was deposited after airborne transportation, which is the formation process of tuff. Tuff is often massive because it formed by falling of fine-grained volcanic material (Fig. 5o). However, some of the tuffaceous material experienced reworking by water flow during or after its deposition, as indicated by weak horizontal bedding (Figs. 5p and 11e-f), which is named reworked tuff.

4.2.12. Dolomitic tuff. Just like tuffaceous dolomite, dolomitic tuff is uncommon due to the infrequent mixing of dolomite and volcanic material. This type of lithological assemblage usually formed when clastic input was limited. Some dolomite does occur in tuff or reworked tuff (Fig. 11b–d, Fig. 11g and h) because the Ca^{2+} and Mg^{2+} ions derived from the solution of neutral-basic volcanic material may have benefited the formation of dolomite ($CaMg(CO_3)_2$). Dolomite crystals in dolomitic tuff are mud-sized (Fig. 11g and h). The main types of mineral components in dolomitic tuff are similar to those of tuffaceous dolomite, just the mineral contents are different.

XRD data show that the sum of quartz, K-feldspar and plagioclase is 66%. The content of carbonate components is nearly 20%, and the average content of clay minerals is 11.6% (Fig. 9).

4.2.13. Silty tuff. Compared with tuffaceous siltstone, volcanic tuffaceous material is the more dominant source when silty tuff deposited. The silty grains brought by rivers are mainly subangular quartz, feldspar and lithic debris, mixed with some amorphous volcanic tuffaceous materials (Fig. 11i). A few grains of calcite and ankerite which formed during diagenesis can be seen in silty tuff. The average content of quartz and feldspar in silty tuff is very high, nearly 75% according to the XRD data. In addition, calcite, ankerite, clay minerals and a small amount of siderite have been detected (Fig. 9). This type of rock experienced slight water flow, shown by weak horizontal bedding (Fig. 11i).

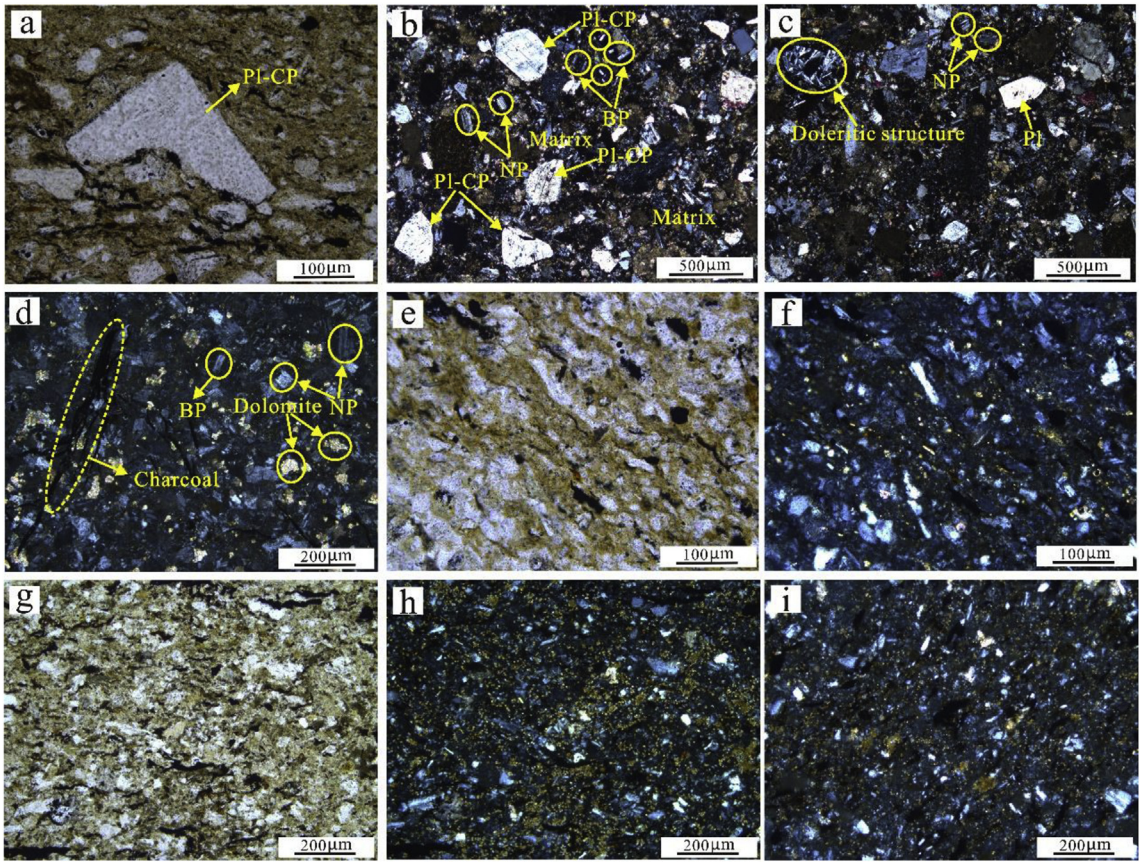

Fig. 11. Photomicrographs of components and textures of different tuffaceous-dominated mixed rocks in the Lucaogou Formation, Jimusaer Sag. In brackets after the description are the well number, section, and depth in core. (PPL = plane-polarized light; CPL = cross-polarized light; Pl = plagioclase; Pl-CP = plagioclase crystal pyroclast; NP = plagioclase in neutral magma; BP = plagioclase in basic magma) (a) tuff, plagioclase crystal pyroclast with clear and intact edge, PPL, (J176, P_2l_2, 3030.3m); (b) tuff, the plagioclase in both crystal pyroclast and matrix kept its euhedral form as lath-shaped and acicular crystals, CPL, (J251, P_2l_2, 3629.45m); (c) tuff, doleritic structure of basic extrusive cuttings, CPL, (J251, P_2l_2, 3629.45m); (d) tuff with charcoal, plagioclase microcrystal form neutral and basic magma in matrix, CPL, (J32, P_2l_1, 3724.91m); (e) reworked tuff, slightly layered, PPL, (J31, P_2l_2, 2717.9m); (f) reworked tuff, same as (e), CPL, (J251, P_2l_1, 3749.86m); (g) dolomitic tuff, PPL, (J32, P_2l_2, 3572.13m); (h) dolomitic tuff, same as (g), CPL, (J32, P_2l_2, 3572.13m); (i) silty tuff, CPL, (J32, P_2l_2, 3568m).

5. Discussion

5.1. Mixing processes of three-component mixed rocks

The four mixing processes defined by Mount (1984) for two-component systems can also be recognized in the three-component mixing system of the Lucaogou Formation, but they are expanded here to account for the addition of volcanic materials.

5.1.1. Facies mixing

Facies mixing takes place where sediments are mixed along the diffuse boundaries between facies (Mount, 1984), for both two and three component systems. It is the most common mixing process in both the lower and upper sections of the Lucaogou Formation in this area. The typical lithological assemblage is lithic arkosic fine sandstone, calcareous/dolomitic fine sandstone, siltstone, dolomitic/calcareous siltstone, silty dolomite/limestone and dolomicrite, which are interpreted to have been deposited, in this order, from distal end of the delta front to shallow lake (Fig. 12a). Thus, this order indicates lateral changes caused by facies mixing. Generally, the nearer to the delta sedimentation takes place, the higher the content of the siliciclastic component is. Conversely, if it is nearer to the shallow lake shore, there is more dolomite or limestone. This lateral change leads to the vertical succession shown in Fig. 12a due to changes in clastic input and/or shifting of river mouths. This type of mixing has been found in Wells J174, J32, J30, J33 and J36 in the lower section (Fig. 13a), and in Wells J174, J32, J176, J31, J251 and J23 in the upper section (Fig. 13b). Generally, facies mixing tends to develop mostly in the delta front to lake shore zone (between the highest lake level and the lowest lake level) and shallow lake environment (where is between the lowest lake level and the wave base) (Fig. 14a), which are transitional from a terrigenous source area to a carbonate production area.

5.1.2. Source mixing

The cause of source mixing in mixed siliciclastic-carbonate rocks is that “the uplift and erosion of lithified carbonate terranes supplies abundant clastic carbonate into the depositional systems dominated by siliciclastic sediments” (Mount, 1984). Source mixing is not due to in situ production of carbonates and is unrelated to basinal dynamics or the local paleoecology (Dorsey and Kidwell, 1999). During the deposition of the Lucaogou Formation, carbonate parent rocks were rare in the area around the lake, and all the carbonate components found here are intrabasinal. Therefore, source mixing of siliciclastic and carbonate rocks is hardly found. In the depositional system with three end-member components of the Lucaogou Formation, source mixing is instead due to the intermingling of tuffaceous and terrigenous material. The tuffaceous material came from the volcanic edifices in the Beisantai Uplift (Fig. 1). It was mostly transported by wind, but some tuff was later reworked by water flow, and then distributed throughout the lacustrine basin when the Lucaogou Formation deposited. As a result of this type of source mixing, dark mudstones, dolomitic mudstone and silty mudstone interbedded with thin layers of tuff, reworked tuff, and

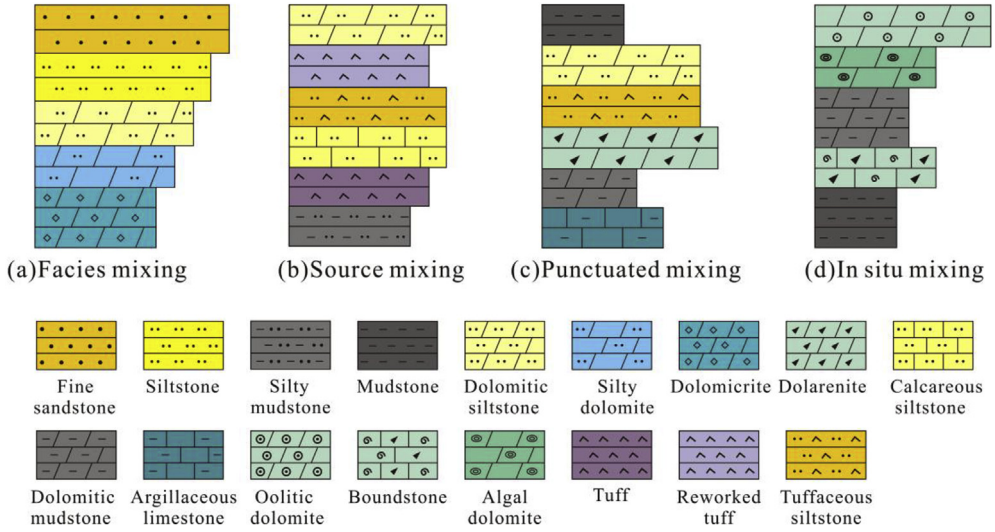

Fig. 12. Lithological associations of different sedimentary mixing processes of the Lucaogou Formation, Jimusaer Sag. See main text for further description.

some tuffaceous siltstones are found near the center of the lacustrine basin. Near and in the shore zone environment, it is more common to find dolomitic/calcareous siltstone, tuffaceous siltstone, and dolomicrite intermixed with reworked tuff and tuff (Fig. 12b).

In the lower section of the Lucaogou Formation, the lithological association caused by source mixing consists of dolomitic siltstone, reworked tuff, tuffaceous siltstone, calcareous siltstone, tuff and dolomitic/silty mudstone (Fig. 12b). The specific order of different lithologies is not very important in the case of source mixing here as it depends on timing of independent processes (volcanic eruptions and terrigenous supply). In summary, source mixing in the lower section of the Lucaogou Formation resulted in the mixing of tuffaceous material (mainly tuff and reworked tuff), and different types of siltstones and mudstones. Compared with the lower section, there are fewer tuffaceous-dominated rocks and terrigenous siltstones in the upper section ($P_2l_2^2$), but more carbonate-dominated rocks and source mixing was less common in the upper part. The resulting lithological assemblage consists mainly of dolomicrite, dolarenite, silty dolomite, dolomitic mudstone and mudstone, mixed with tuffaceous siltstones, and a minor amount of tuff, reworked tuff and dolomitic tuff. Deposits resulting from source mixing have been found in Wells J251, J32, J37, J176 and J36, which are distributed widely in delta front and shore lake environments. Source mixing developed mostly near the edge of the lake, where terrigenous material was supplied from land, and then mixed with tuffaceous material.

5.1.3. *Punctuated mixing*

Punctuated mixing is always related to event deposition (Ager, 1981; Mount, 1984), and this mixing process may be caused by storm surges, gravity flow, floods or delta front collapses. It provides a mechanism for the sporadic transportation of nearshore siliciclastic sediments into deeper, but still carbonate-dominated environments, or of carbonate rocks into deeper environments where mudstones form the main deposits. In this case, the fine sandstones have a sharp contact with the underlying carbonate-dominated mixed rocks or (dolomitic) mudstones (Fig. 5k), and they often develop massive bedding or graded bedding, reflecting rapid sedimentation. Punctuated mixing may also cause erosion of carbonates and transport carbonate clasts landwards and redeposit them in a more siliciclastic-dominated environment (Kreisa, 1981). This type of mixing in the Lucaogou Formation is relatively infrequent. In both the lower and upper sections, punctuated mixing tends to occur in deeper environments. Here, dolomitic fine sandstone, dolomitic siltstone, tuffaceous siltstone were brought down from the delta front and lake shore, or dolarenite and dolomitic siltstone from shallower parts of the lake. Storms, flooding and gravity flows etc., deposited these coarse grains together with the fine-grained

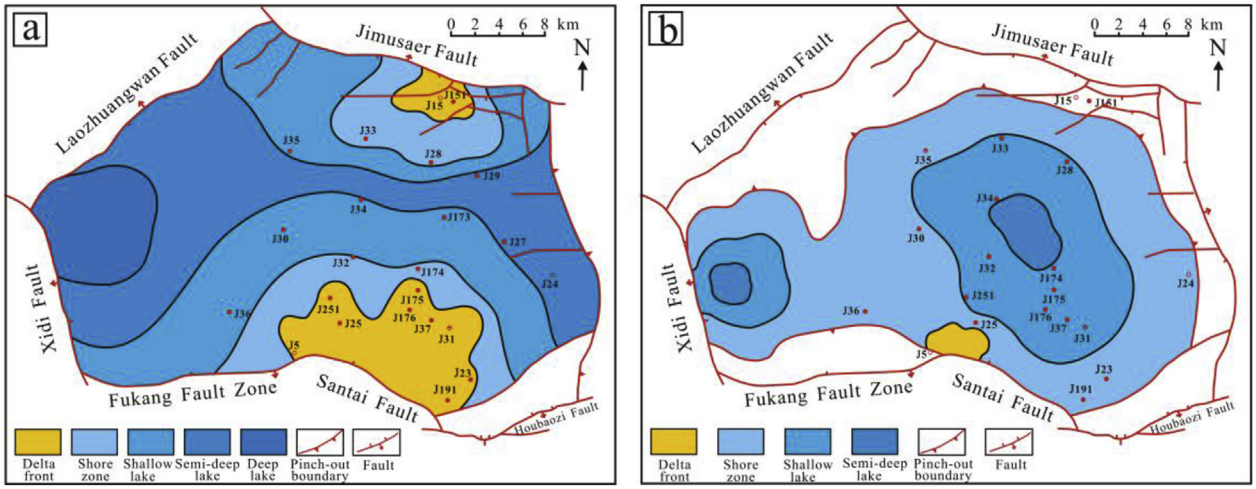

Fig. 13. The depositional environment distributions of the lower and upper sections of the Lucaogou Formation, Jimusaer Sag. The interpretation in the western part of the lake is speculative, due to the lack of core data. (a) the lower section; (b) the upper section.

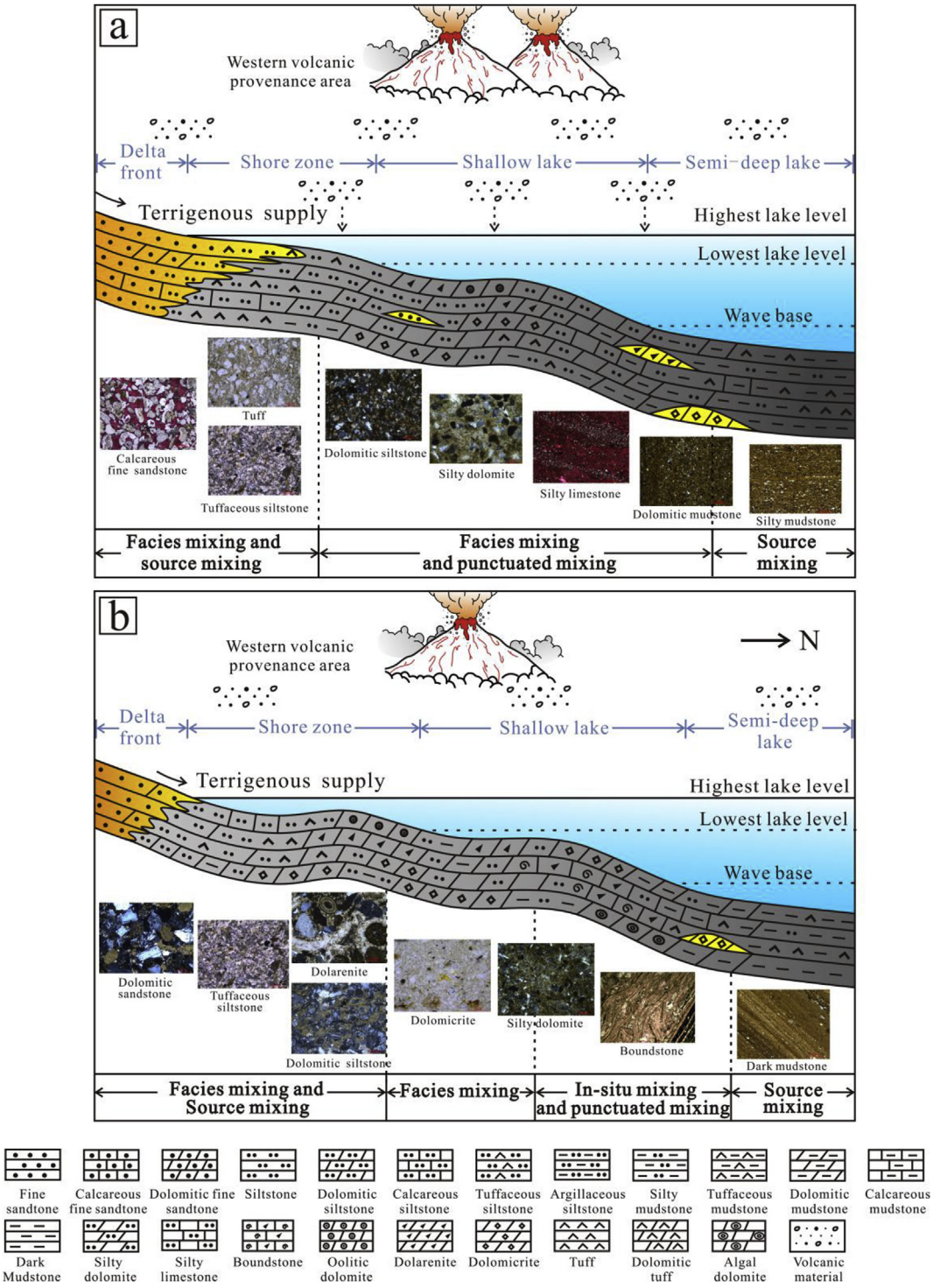

Fig. 14. Depositional models and mixing processes of the lower and upper sections in the Lucaogou Formation, Jimusaer Sag (a) lower section (b) upper section.

dolomitic mudstone, mudstone or argillaceous limestone of the deeper water environment (Fig. 12c). The vertical sedimentary succession caused by punctuated mixing is shown in Fig. 12c. Deposits interpreted to have been formed by punctuated mixing have been found in Wells J30, J35, J174 and J36 laterally in the Jimusaer Sag, generally at intermediate depths and in deeper parts of the lake.

5.1.4. In-situ mixing

Generally, in situ mixing is the process of mixing of autochthonous or parautochthonous death assemblages of calcareous organisms with terrigenous mud (Mount, 1984). This mixing process involves the formation of mixed sediments locally (hence the name), rather than lateral transfer from one facies to another (Mount, 1984; Zhang, 2000). This in situ mixing process tends to develop in shallow to semi-deep water environments, and the lithological assemblage is often boundstone, terrigenous mudstone and siltstone in the Lucaogou Formation. Algal dolomite/limestone occurs here sometimes because the algae can produce calcareous carbonates as well as trap and bind clastic material, leading to the local formation of mixed rocks. An additional source composed of bioclasts, ooids and some intraclasts usually formed in

high-energy environments where lake waves caused erosion and transportation of semi-consolidated or consolidated carbonate sediments. Due to this reworking, the carbonate-rich intraclasts mixed with a siliciclastic matrix (Sepkoski, 1982). Therefore, oolitic dolomite, algal dolomite, (dolomitic) mudstone, boundstone and some siltstones can be found in the in situ mixing process, as shown in the lithological section in Fig. 12d. In situ mixing occurred relatively little when the Lucaogou Formation deposited in the Jimusaer Sag, but it can be seen in wells J30, J34, J174 and J36, which are from quiet and low-energy environments, with intermittent high energy disturbances.

5.2. Effect of environment on mixed sedimentation

Mixed siliciclastic-carbonate sedimentation is controlled by many factors. In previous studies, climate change, sea or lake level fluctuation, tectonic activity and sediment supply rate were considered to be the most important influences affecting mixed sedimentation (Einsele, 1996; Zhang and Ye, 1989; Wright et al., 2005; Gischler et al., 2010; Zheng et al., 2015). The role of energy levels of the different environments has not been included explicitly, even though the type of mixing process taking place depends on the depositional environment, and thus at least partly on the energy levels in that environment.

The fine sandstones contain carbonate clasts that have been transported into the area where the sandstones were deposited, but do not contain carbonates developed in situ. They can also contain calcite cement and replacement dolomite, but these formed during diagenesis, not during deposition, so they are not part of the mixed sedimentation.

Siltstones and mudstones, unlike the fine sandstones, can be mixed with in-situ carbonates. These rocks were deposited away from the main clastic input at river mouths, under generally more quiescent conditions than the sandstones, with the mudstones deposited under the most quiescent conditions. These quieter lake conditions allowed the formation of the carbonate muds found in the lake.

Grain size frequency distribution curves show that the peaks of fine sandstone are narrow (Fig. 7a and b), indicating an energy level where fine-grained carbonate mud could not deposit, thus preventing in situ mixing. The grain size curves of the different types of siltstone are much broader (Fig. 7c–f), and include both grains larger and smaller than silt. This indicates that siltstones were deposited under conditions of variable energy levels, allowing for more types of mixing processes than the sandstones.

The tuffaceous component was not so strongly influenced by the different energy levels in the lake as it was often brought in by wind and was thereby spread reasonably uniformly across the lake. Tuff was mainly influenced by environmental energy levels when being reworked.

5.3. Changes of sedimentary facies and depositional environment through time

The sedimentary environments and energy levels when the Lucaogou Formation deposited varied considerably, as seen in the cores (Figs. 5–6, Figs. 10–11). This variation was caused by a number of different processes, some of which were due to external influences of the lake level fluctuations.

In general, the Lucaogou Formation consists of two lacustrine regression-transgression cycles (Fig. 3, see also Wu et al., 2016). When deposition of section $P_2l_1^2$ started, the sedimentary environment varied from shallow to semi-deep lake (Figs. 3 and 13a). With the falling of the lake level, large scale mixed sedimentation developed in the shore and shallow lacustrine environments, with some deposition taking place in a delta front. At that time, large amounts of siltstone, dolomitic/calcareous siltstone, argillaceous siltstone, tuffaceous siltstone, tuff, silty tuff, reworked tuff were interbedded with dolomicrite, dolarenite and thin layers of fine sandstone, mudstone, tuffaceous mudstone, silty mudstone and dolomitic/calcareous mudstone. Subsequently the lake level rose, resulting in the deposition of thick mudstones in section $P_2l_1^1$, with some dolomitic mudstones, silty mudstones and lime mudstones in shallow to semi-deep lacustrine environments (Fig. 3). Later, during deposition of section $P_2l_2^2$, the lake level started to fall again, and the depositional environment varied from shallow to semi-deep lake to shore zone and shallow lake (Figs. 3 and 13b). During that time, a large amount of dolomicrite, dolarenite, silty dolomite, dolomitic/silty limestone deposited, interbedded with tuffaceous siltstone/mudstone, boundstone, oolitic dolomite, algal dolomite, dolomitic tuff and reworked tuff. Finally, during deposition of section $P_2l_2^1$, the lake level rose again and fine-grained rocks such as dolomitic mudstone, silty mudstone, argillaceous siltstone, dark mudstone and tuffaceous mudstone developed. Throughout the entire Lucaogou Formation, mixed sedimentation developed mainly in the upper part of $P_2l_2^2$ and $P_2l_1^2$, during periods of low lake level, while fine-grained sedimentary rocks (many types of mudstones) developed between them, during periods of high lake level (Fig. 3).

5.4. Mixed depositional models of saline lacustrine basin

Overall, the mixed sedimentation of the Lucaogou Formation is a multi-source depositional system. The mixed sedimentary rocks mainly developed in distal end of delta front, shallow lake and shore zone environments. The latter was periodically dry, and thus experienced evaporation. Facies mixing was the most widely distributed mixing process in both the lower and upper sections of the Lucaogou Formation. Punctuated mixing and source mixing tended to develop more in the lower section, while in-situ mixing developed more in the upper section (Figs. 3 and 14).

Mixed sedimentation in the lower section was controlled by terrigenous and volcanic material supply, lake level fluctuation leading to frequent variations of lithology and energy level, as discussed above. After deposition of a thick mudstone, the upper section was deposited in shore zone to shallow lacustrine environments, and the external source input decreased. The key controlling factors of mixed sedimentation of the upper section were climate variation (see also Hackley et al., 2016; Wu et al., 2016), lake level fluctuation and energy environment. Although alternating single layers of different lithologies occur frequently throughout the entire Lucaogou Formation, there are differences between the lower and upper sections in the sedimentary facies, lithological assemblages of mixed rocks and sedimentary mixing processes.

5.4.1. Depositional model of the lower section of the Lucaogou Formation

The lower section consists mainly of fine-grained terrigenous clastic rocks (mostly siltstones, part of fine sandstones and mudstones), some tuffaceous rocks and carbonate rocks. When the lower section ($P_2l_2^1$) deposited, terrigenous clastics constant influx from rivers resulted in a large area of deltaic deposits (Fig. 13a), which suppressed carbonate formation. The terrigenous supply came predominantly from a southern provenance, while a northern source was much smaller (Si et al., 2013; Kuang et al., 2015). Therefore, the deltaic sand body mostly stretched out from south to north until pinching out (Fig. 13a). In the southern delta system, fine sandstones or siltstones developed with intermittent thin layers of reworked tuff (Fig. 14a). Tuff, silty tuff and reworked tuff were deposited widely in section $P_2l_1^2$ (Jiang et al., 2015; Xi et al., 2015) as a result of volcanic activity around the basin. Consequently it was easy to get source mixing when the tuffaceous material admixed with terrigenous detrital material such as fine sandstones, siltstones and mudstones (Figs. 13b and 14a). From the edge to the center of the lacustrine basin, the sedimentary environment changed from delta front to semi-deep lake gradually, and the mixing process along this transect was mainly facies mixing. The main lithologies changed from fine sandstone, dolomitic/calcareous siltstones and tuffaceous siltstones to silty dolomite and dolomitic mudstones, with thin interlayers of tuff, reworked tuff, silty tuff, dolomicrite and dolarenite. Additionally, gravity flow deposits caused by storm surges, wind forcing, flooding

episodes or delta front instability brought siliciclastic sediments in shallow part into the carbonate-dominated or mud-dominated deeper environment, resulting in punctuated mixing. In the semi-deep lacustrine environment, the amount of carbonate minerals decreased, and the main lithologies were silty mudstones, dolomitic mudstone and dark mudstones. Some tuffaceous material was also added and resulted in source mixing. The depositional model of mixed sedimentation in the lower section is summarized in Fig. 14a.

5.4.2. Depositional model of the upper section of the Lucaogou Formation

During the deposition of the upper section ($P_2l_2^2$), the input of terrigenous clastics and volcanic material declined. At the same time, the lake water tended to have higher salinity (Wu et al., 2016), resulting in the formation of more dolomite. Therefore, more carbonate-dominated rocks, and fewer terrigenous-dominated rocks and tuffaceous-dominated rocks are present in section $P_2l_2^2$ (Fig. 3). The lithologies of the upper part are more varied than those of the lower section, and include dolomitic siltstone, dolomicrite, silty dolomite, silty limestone, dolarenite and dolomitic mudstones, with small amounts of dolomitic tuff, reworked tuff, tuffaceous mudstone, boundstone, algal dolomite and oolitic dolomite. The distribution of the delta front deposits is less widespread, but the assemblage formed by facies mixing in the upper section is similar to that in the lower. Shore lake deposits developed between the highest and lowest lake levels, where dolomitic siltstones, silty dolomite, dolarenite and dolomicrite alternated. A calcareous beach often developed at the shore. At the same time in the shore lake, small amounts of tuffaceous material mixed with terrigenous detrital particles, resulting in source mixing. Some autochthonous boundstone and algal dolomite formed in the shallow lake to semi-deep lake within silty mudstones, dolomitic mudstones and mudstones, resulting in in-situ mixing. On the whole, the deposition of the upper section was dominated by facies mixing, while source mixing and in-situ mixing occurred locally (Fig. 14b).

6. Conclusions

The Lucaogou Formation in the Jimusaer Sag, Junggar Basin is a set of siliciclastic-carbonate-tuffaceous mixed rocks deposited in a saline lake. This new type of mixed rocks has been classified into three categories based on core description, thin section description, and grain size measurements, with nine subtypes according to the proportion of the three end-member components of terrigenous clastics, carbonates, and volcanic material. More than 20 lithologies have been recognized. The main lithologies are pebbly fine sandstone, calcareous/dolomitic fine sandstone, argillaceous siltstone, dolomitic/calcareous siltstones, tuffaceous siltstone, silty mudstone, calcareous/dolomitic mudstone, dark mudstone, boundstone, silty dolomite/limestone, dolomicrite, dolarenite, tuff, reworked tuff, dolomitic tuff and silty tuff, etc. The lithological assemblages are different in the lower and upper sections of the formation. The lower section contains more terrigenous-dominated and tuffaceous-dominated mixed rocks, but fewer carbonate-dominated mixed rocks than the upper section. The mixing processes of the three end-member component mixed rocks can be divided into the four general categories of facies mixing, source mixing, punctuated mixing and in-situ mixing proposed by Mount (1984), but their descriptions have been expanded for the multi-source mixed sedimentary system in the Lucaogou Formation. Facies mixing occurred most widely during deposition of both the lower and upper sections; source mixing and punctuated mixing were more common during deposition of the lower section, while in-situ mixing tended to occur more during deposition of the upper section. The controlling factors on mixed sedimentation included climate change, lake level fluctuation, tectonic activity and sediment supply rate, and energy level of the depositional environments. Based on analyses of lithological assemblage, sedimentary facies, and mixing processes and energy environment, different mixed depositional models have been established for the lower and upper sections.

Acknowledgments

This study was supported by the National Natural Science Foundation of China, China Project entitled “Effectiveness of micro-nano pore throat system to oil charging in tight sandstone and its control on oil accumulation” (Project No. 41472114), and the National Science and Technology Major Project, China “The Accumulation Law and Key Technologies for Exploration and Exploitation of Tight Oil” (Grant No:2016ZX05046). We also would like to thank Xinjiang Oilfield for providing the core samples and logging data. Additionally, we are grateful to Professor Zhong Dakang for the constructive comments on the revision of this manuscript. The first author stayed at NTNU during the final preparation of this article and wants to thank Porelab, Norway, through their Center of Excellence funding scheme (Project No. 262644), for their support.

Appendix A. Supplementary data

Supplementary data to this article can be found online at https://doi.org/10.1016/j.marpetgeo.2019.01.016.

References

Accordi, G., Carbone, F., 2016. Evolution of the siliciclastic-carbonate shelf system of the northern Kenyan coastal belt in response to Late Pleistocene-Holocene relative sea level changes. J. Journal of African Earth Sciences. 123, 234–257.
Amireh, B.S., 2015. Grain size analysis of the Lower Cambrian–Lower Cretaceous clastic sequence of Jordan, sedimentological and paleo-hydrodynamical implications. J. Journal of Asian Earth Sciences. 97, 67–88.
Brooks, G.R., Doyle, L.J., Suthard, B.C., Locker, S.D., Hine, A.C., 2003. Facies architecture of the mixed carbonate/siliciclastic inner continental shelf of west-central Florida, implications for Holocene barrier development. J. Marine Geology. 200 (1–4), 325–349.
Bruckner, W.D., 1953. Cyclic calcareous sedimentation as an index of climatic variations in the past. J. Journal of Sedimentary Research. 23, 235–237.
Button, A., Vos, R.G., 1977. Subtidal and intertidal clastic and carbonate sedimentation in a macrotidal environment, an example from the lower Proterozoic of South Africa. J. Sedimentary Geology 18, 175–200.
Cao, Z., Liu, G., Kong, Y., Wang, C., Niu, Z., Zhang, J., Geng, C., Shan, X., Wei, Z., 2016. Lacustrine tight oil accumulation characteristics, permian Lucaogou Formation in jimusaer sag, Junggar Basin. J. International Journal of Coal Geology 153, 37–51.
Cao, Z., Liu, G., Zhan, H., Gao, J., Zhang, J., Li, C., Xiang, B., 2017a. Geological roles of the siltstones in tight oil play. J. Marine and Petroleum Geology 83, 333–344.
Cao, Z., Liu, G., Xiang, B., Wang, P., Niu, G., Niu, Z., Li, C., Wang, C., 2017b. Geochemical characteristics of crude oil from a tight oil reservoir in the Lucaogou Formation, Jimusar sag, Junggar Basin. J. Aapg Bulletin. 101 (1), 39–72.
Caracciolo, L., Gramigna, P., Critelli, S., Calzona, A.B., Russo, F., 2013. Petrostratigraphic analysis of a Late Miocene mixed siliciclastic–carbonate depositional system (Calabria, Southern Italy), implications for mediterranean paleogeography. J. Sedimentary Geology 284, 117–132.
Choi, D.R., Ginsburg, R.N., 1982. Siliciclastic foundations of Quaternary reefs in the southernmost Belize Lagoon, British Honduras. J. Geological Society of America Bulletin. 93 (2), 116–126.
Christiansen, C., Blaesild, P., Dalsgaard, K., 1984. Re-interpreting ‘segmented’ grain-size curves. J. Geological Magazine. 121 (1), 47–51.
Ding, Y., Li, Z.W., Feng, F., et al., 2013. Mixing of lacustrine siliciclastic-carbonate sediments and its significance for tight oil exploration in the Daanzhai Member, Ziliujing Formation, lower Jurassic, in Longgang area, central Sichuan Basin. J. Geological Review 59 (2), 389–400.
Dong, G.Y., Chen, H.D., Li, J.W., et al., 2009. The cambrian mixed sedimentation around bohai sea bay basin. J. Acta Geologica Sinica. 83 (6), 800–811.
Dong, G.Y., He, Y.B., Chen, H.D., et al., 2007. Mixed sedimentation of carbonates of lagoonal facies and terrigenous clastics of the middle Submember of member 1 of Shahejie Formation in Huiming Sag, taking Shanghe area in Shandong province for an example. J. Acta Sedimentologica Sinca. 25 (3), 343–350 (in Chinese with English abstract).
Dorsey, R.J., Kidwell, S.M., 1999. Mixed carbonate-siliciclastic sedimentation on a tectonically active margin, Example from the Pliocene of Baja California Sur, Mexico. J. Geol. 27 (10), 935–938.
Einsele, G., 1996. Event deposits, the role of sediment supply and relative sea-level changes—overview. J. Sedimentary Geology. 104 (1–4), 11–37.
Escalona, N., Abud, J., 1989. Reservoir heterogeneity and hydrocarbon production in mixed dolomitic-clastic sequence, Escandalosa Formation, Barinas-Apure basin, southwestern Venezuela. J. AAPG Bulletin, (United States) 73 (CONF-890404-).
Feng, J., Cao, J., Hu, K., et al., 2013. Dissolution and its impacts on reservoir formation in moderately to deeply buried strata of mixed siliciclastic-carbonate sediments, northwestern Qaidam Basin, northwest China. J. Marine & Petroleum Geology 39 (1), 124–137.
Flood, P.G., Orme, G.R., 1988. Mixed siliciclastic/carbonate sediments of the northern

Great Barrier Reef province, Australia. J. Developments in Sedimentology. 42, 175–205.
Folk, R.L., Ward, W.C., 1957. Brazos River bar, a study in the significance of grain size parameters. J. Journal of Sedimentary Research 27 (1), 3–26.
Folk, R.L., 1966. A review of grain-size parameters. J. Sedimentology. 6 (2), 73–93.
Friedman, G.M., Sanders, JE., 1978. Principles of Sedimentology. M. Wiley.
Fu, Q.L., Qing, H.R., Bergman, K.M., 2006. Early dolomitization and recrystallization of carbonate in an evaporite basin, the Middle Devonian Ratner laminite in southern Saskatchewan, Canada. J. Journal of the Geological Society 163 (11), 937–948.
García-Hidalgo, J.F., Gil, J., Segura, M., et al., 2007. Internal anatomy of a mixed siliciclastic–carbonate platform, the Late Cenomanian–Mid Turonian at the southern margin of the Spanish Central System. J. Sedimentology. 54 (6), 1245–1271.
Ghoshal, K., Mazumder, B.S., Purkait, B., 2010. Grain-size distributions of bed load, Inferences from flume experiments using heterogeneous sediment beds. J. Sedimentary Geology. 223 (1–2), 1–14.
Gischler, E., Ginsburg, R.N., Herrle, J.O., et al., 2010. Mixed carbonates and siliciclastics in the Quaternary of southern Belize, Pleistocene turning points in reef development controlled by sea-level change. J. Sedimentology. 57 (4), 1049–1068.
Gregg, J.M., Shelton, K.L., 1990. Dolomitization and dolomite neomorphism in the back reef fades of the Bonneterre and Davis Formations (Cambrian), southeast Missouri. J. Journal of Sedimentary Research 60 (4), 549–562.
Hackley, P.C., Fishman, N., Wu, T., et al., 2016. Organic petrology and geochemistry of mudrocks from the lacustrine Lucaogou Formation, Santanghu Basin, northwest China, Application to lake basin evolution. J. International Journal of Coal Geology 168, 20–34.
Hatch, T., Choate, S.P., 1929. Statistical description of the size properties of non uniform particulate substances. J. Journal of the Franklin Institute. 207 (3), 369–387.
Holmes, C.W., 1983. Carbonate and siliciclastic deposits on slope and abyssal floor adjacent to southwestern Florida platform. J. AAPG Bulletin. 67 (3), 484–485.
Huang, Z., Yang, S., Chen, Z., 1997. Mineralogical correlation between primary and replacement dolomites. J. Science in China Series D, Earth Sciences 40 (1), 91–98.
Inman, D.L., 1952. Measures for describing the size distribution of sediments. J. Journal of Sedimentary Research 22 (3), 125–145.
Isaack, A., Gischler, E., Hudson, J.H., et al., 2016. A new model evaluating Holocene sediment dynamics, Insights from a mixed carbonate–siliciclastic lagoon (Bora Bora, Society Islands, French Polynesia, South Pacific). J. Sedimentary Geology 343, 99–118.
Jiang, Y.Q., Liu, Y.Q., Yang, Z., et al., 2015. Characteristics and origin of tuff-type tight oil in jimusar depression, Junggar Basin, NW China. Petrol. Explor. Dev. 42 (06), 741–749 (in Chinese with English abstract).
Konert, M., Vandenberghe, J.E.F., 1997. Comparison of laser grain size analysis with pipette and sieve analysis, a solution for the underestimation of the clay fraction. J. Sedimentology. 44 (3), 523–535.
Kreisa, R.D., 1981. Storm-generated sedimentary structures in subtidal marine facies with examples from the Middle and Upper Ordovician of southwestern Virginia. J. Journal of Sedimentary Research 51 (3), 823–848.
Krumbein, W.C., 1938. Size frequency distributions of sediments and the normal phi curve. J. Journal of Sedimentary Research. 8 (3), 84–90.
Kuang, L.C., Tang, Y., Lei, D.W., et al., 2012. Formation conditions and exploration potential of tight oil in the Permian saline lacustrine dolomitic rock, Junggar Basin, NW China. Petrol. Explor. Dev. 39 (6), 657–667 (in Chinese with English abstract).
Kuang, L.C., Hu, W.X., Wang, X.L., et al., 2013. Research of the tight oil reservoir in the Lucaogou Formation in Jimusar Sag, analysis of lithology and porosity characteristics. J. Geological Journal of China Universities 19 (03), 529–535 (in Chinese with English abstract).
Kuang, L.H., Wang, X.T., Guo, X.G., et al., 2015. Geological characteristics and exploration practice of tight oil of Lucaogou Formation in jimsar sag. J. Xinjiang Petroleum Geology 36 (6), 629–634.
Li, X.H., 2008. Mixing of siliciclastic-carbonate sediments within systems tracts of depositional sequences and its controlling factors. J. Geological Journal of China Universities 14 (3), 395–404.
Loyd, S.J., Corsetti, F.A., 2010. The origin of the millimeter-scale lamination in the neoproterozoic lower beck spring dolomite, implications for widespread, fine-scale, layer-parallel diagenesis in precambrian carbonates. J. Journal of Sedimentary Research 80 (7), 678–687.
Lubeseder, S., Redfern, J., Boutib, L., 2009. Mixed siliciclastic-carbonate shelf sedimentation—lower Devonian sequences of the SW Anti-Atlas, Morocco. J. Sedimentary Geology. 215 (1–4), 13–32.
Mack, G.H., James, W.C., 1986. Cyclic sedimentation in the mixed siliciclastic-carbonate Abo-Hueco transitional zone (Lower Permian), southwestern New Mexico. J. Journal of Sedimentary Research 56 (5), 635–647.
Mao, X., Li, J.H., Zhang, H.T., et al., 2012. Study on the distribution and developmental environment of the Late Paleozoic volcanoes in Junggar Basin and its adjacent areas. J. Acta Petrologica Sinica. 28 (7), 2381–2391 (in Chinese with English abstract).
McIlreath, I.A., Ginsburg, R.N., 1982. Mixed deposition of carbonate and siliciclastic sediments. Int. Sedimentol. Congress., IAS. J. Symposium. 27, 109–113.
Mount, J.F., 1984. Mixing of siliciclastic and carbonate sediments in shallow shelf environments. J. Geol. 12 (7), 432–435.
Nichols, G., 2009. Sedimentology and stratigraphy[M]. John Wiley & Sons.
Orpin, A.R., Brunskill, G.J., Zagorskis, I., et al., 2004. Patterns of mixed siliciclastic-carbonate sedimentation adjacent to a large dry-tropics river on the central Great Barrier Reef shelf, Australia. J. Australian Journal of Earth Sciences 51 (5), 665–683.
Page, M.C., 2006. Late Pleistocene-Holocene Deposition of Mixed Siliciclastic-Carbonate Sediments on Slopes East of the Great Barrier Reef, Northeast Australian Margin. Doctoral dissertation. James Cook University.
Palermo, D., Aigner, T., Geluk, M., et al., 2008. Reservoir potential of a lacustrine mixed carbonate/siliciclastic gas reservoir, the lower triassic rogenstein in The Netherlands. J. Journal of Petroleum Geology 31 (1), 61–96.
Peng, Y., Xiao, J., Nakamura, T., et al., 2005. Holocene East Asian monsoonal precipitation pattern revealed by grain-size distribution of core sediments of Daihai Lake in Inner Mongolia of north-central China. J. Earth and Planetary Science Letters 233 (3), 467–479.
Pilkey, O.H., Bush, D.M., Rodriguez, R.W., 1988. Carbonate-terrigenous sedimentation on the north Puerto Rico shelf. J. In Developments in Sedimentology 42, 231–250.
Purdy, E.G., Gischler, E., 2003. The Belize margin revisited, 1. Holocene marine facies. J. International Journal of Earth Sciences 92 (4), 532–551.
Qiu, Z., Tao, H., Zou, C., et al., 2016. Lithofacies and organic geochemistry of the middle permian Lucaogou Formation in the jimusar sag of the Junggar Basin, NW China. J. Petrol. Sci. Eng. 140, 97–107.
Reis, H.L.S., Suss, J.F., 2016. Mixed carbonate-siliciclastic sedimentation in forebulge grabens, an example from the ediacaran bambuí group, são francisco basin, Brazil. J. Sedimentary Geology 339, 83–103.
Roux, J.P.L., Rojas, E.M., 2007. Sediment transport patterns determined from grain size parameters, Overview and state of the art. J. Sedimentary Geology. 202 (3), 473–488.
Sepkoski, J.J., 1982. Flat-Pebble Conglomerates, Storm Deposits, and the Cambrian Bottom Fauna. M. Cyclic and Event Stratification. Springer Berlin Heidelberg, pp. 371–385.
Shao, Y., Yang, Y.Q., Wan, M., et al., 2015. Sedimentary characteristic and facies evolution of permian Lucaogou Formation in jimsar sag, Junggar Basin. J. Xinjiang Petroleum Geology 36 (6), 635–641 (in Chinese with English abstract).
Si, C.S., Chen, N.G., Yu, C.F., et al., 2013. Sedimentary characteristics of tight oil reservoir in permian Lucaogou Formation, jimsar sag. J. Petroleum Geology and Experiment. 35 (05), 528–533 (in Chinese with English abstract).
Sibley, D.F., Gregg, J.M., 1987. Classification of dolomite rock textures. J. Journal of Sedimentary Petrology 57 (6), 967–975.
Stapor, F.W., Tanner, W.F., 1975. Hydrodynamic implications of beach, beach ridge and dune grain size studies. J. Journal of Sedimentary Research. 45 (4), 926–931.
Testa, V., Bosence, D.W.J., 1999. Physical and biological controls on the formation of carbonate and siliciclastic bed forms on the north-east Brazilian shelf. J. Sedimentology. 46 (2), 279–301.
Tirsgaard, H., 1996. Cyclic sedimentation of carbonate and siliciclastic deposits on a late precambrian ramp, the elisabeth bjerg formation (eleonore bay supergroup) east Greenland. J. Journal of Sedimentary Research 66 (4), 699–712.
Visher, G.S., 1969. Grain size distributions and depositional processes. J. Journal of Sedimentary Research 39 (3), 1074–1106.
Wang, D., Chen, D.Z., Yang, C.C., 2010. Classification of texture in burial dolomite. J. Acta Sedimentologica Sinica 28 (1), 17–25.
Wang, G.Z., 2001. Mixed sedimentation of recent reefoid carbonates and terrigenous clastics in the north continental shelf of the South China Sea. J. Journal of Palaegeography 3 (2), 47–54 (in Chinese with English abstract).
Wright, E.E., Hine, A.C., Goodbred, S.L., et al., 2005. The effect of sea-level and climate change on the development of a mixed siliciclastic-carbonate, deltaic coastal, Suwannee River, Florida, USA. J. Sediment. Res. 75, 621–635.
Wu, H., Hu, W., Cao, J., et al., 2016. A unique lacustrine mixed dolomitic-clastic sequence for tight oil reservoir within the middle Permian Lucaogou Formation of the Junggar Basin, NW China, Reservoir characteristics and origin. J. Marine & Petroleum Geology. 76, 115–132.
Xi, K., Cao, Y.C., Zhu, R.K., et al., 2015. Rock types and characteristics of tight oil reservoir in Permian Lucaogou Formation, Jimusaer sag. J. Acta Petroleum Sinica. 36 (12), 1495–1507 (in Chinese with English abstract).
Yang, F., Zou, N.N., Shi, J.A., et al., 2013. Probability cumulative grain size curves in the paleogene clastic sediments and environmental significance in maxian region of northern qaidam basin. J. Natural Gas Geoscience 24 (4), 690–700 (in Chinese with English abstract).
Yose, L.A., Heller, P.L., 1989. Sea-level control of mixed-carbonate-siliciclastic, gravity-flow deposition, Lower part of the Keeler Canyon Formation (Pennsylvanian), southeastern California. J. Geological Society of America Bulletin. 101 (3), 427–439.
Zhang, X.H., 2000. Classification and origin of mixosedimentite. J. Geological Science and Technology Information. 19 (04), 31–34 (in Chinese with English abstract).
Zhang, J.Q., Ye, H.Z., 1989. A study on carbonate and siliciclastic mixed sediments. J. Journal of Chengdu College of Geology 16 (2), 87–92 (in Chinese with English abstract).
Zhao, C., Li, X.B., H, J.L., et al., 2013. Mechanism of mixed siliciclastic-carbonate sediments and its controlling factors. J. Geological Review. 59 (4), 615–626 (in Chinese with English abstract).
Zhao, C.L., Zhu, X.M., 2001. Sedimentary Petrology. M, third ed. Petroleum Industry Press, Beijing.
Zheng, D.S., Cheng, Y., Li, M.L., Wu, W., Zhou, L., Sun, F.B., Wang, P.X., 2015. Sedimentary characteristics and controlling factors of the mixed deposits from the upper member of the Middle Jurassic Ma'ao Formation in the Jiyuan Basin, western Henan. J. Sedimentary Geology and Tethyan Geology 35 (1), 102–108 (in Chinese with English abstract).
Zhu, X.M., 2008. Sedimentary Petrology. M, fourth ed. Petroleum Industry Press, Beijing.